Title Page

Inflammatory Regulation of ABC Efflux Transporter Expression and Function in Microglia

Christopher J. Gibson, Muhammad M. Hossain, Jason R. Richardson, Lauren M. Aleksunes

Department of Pharmacology and Toxicology, Rutgers University Ernest Mario School of Pharmacy, Piscataway, NJ, USA (CJG, LMA, Primary Laboratory of Origin)

Environmental and Occupational Health Sciences Institute, a Joint Institute of Robert Wood Johnson Medical School and Rutgers, The State University of New Jersey, Piscataway, NJ, USA (JRR, LMA)

Department of Environmental and Occupational Medicine, University of Medicine and Dentistry of New Jersey, Piscataway, NJ, USA (MMH, JRR)

JPET Fast Forward. Published on August 31, 2012 as DOI: 10.1124/jpet.112.196543
This article has not been copyedited and formatted. The final version may differ from this version.

Running Title Page

Running Title: Transporter Function in Activated Microglia

Send Correspondence to:

Lauren Aleksunes, Pharm.D., Ph.D., Dept of Pharmacology and Toxicology, Rutgers University, 170 Frelinghuysen Rd. Piscataway, NJ, 08854 USA Phone: (848) 445-5518 Fax: (732) 445-0119 E-mail: aleksunes@eohsi.rutgers.edu

Number of Text Pages: 44
Number of Tables: 2
Number of Supplemental Tables: 1
Number of Figures: 9
Number of Supplemental Figures: 3
Number of Supplemental Figures for Reviewers Only: 2
Number of References: 59
Number of Words in Abstract: 249
Number of Words in Introduction: 586
Number of Words in Discussion: 1500

Non-Standard Abbreviations

ABC, ATP binding cassette; Mdr, multidrug resistance protein; Mrp, multidrug resistance-associated protein; Bcrp, breast cancer resistance protein; LPS, lipopolysaccharide; NF-κB, nuclear factor kappa B; IκB, inhibitor of kappa B; Nrf2, nuclear factor-e2 related factor 2; TNFα, tumor necrosis factor-α; IL, interleukin; BODIPY, boron-dipyrromethene; NBD, nitrobenzoxadiazole; DAPI, 4',6-Diamidino-2-phenylindole; Nqo1, NAD(P)H quinone oxidoreductase 1; NSAID, nonsteroidal anti-inflammatory drugs

Section Assignment Neuropharmacology or Metabolism, Transport, and Pharmacogenomics

JPET Fast Forward. Published on August 31, 2012 as DOI: 10.1124/jpet.112.196543
This article has not been copyedited and formatted. The final version may differ from this version.

Abstract

ATP-binding cassette (ABC) efflux transporters, including the multidrug resistance protein 1 (Mdr1), breast cancer resistance protein (Bcrp), and multidrug resistance-associated proteins (Mrps) extrude chemicals from the brain. While ABC transporters are critical for blood-brain barrier integrity, less attention has been placed on the regulation of these proteins in brain parenchymal cells such as microglia. Prior studies demonstrate that inflammation following lipopolysaccharide (LPS) treatment alters transporter expression in the livers of mice. Here, we sought to determine the effects of inflammation on the expression and function of transporters in microglia. To test this, the expression and function of ABC efflux transport proteins were quantified in mouse BV-2 microglial cells in response to activation with LPS. Intracellular retention of fluorescent rhodamine 123, Hoechst 33342, and calcein AM was increased in LPS-treated microglia suggesting that the function of Mdr1, Bcrp, and Mrps were decreased, respectively. LPS reduced Mdr1, Bcrp, and Mrp4 mRNA and protein expression between 40 and 70%. Conversely, LPS increased expression of Mrp1 and Mrp5 mRNA and protein. Immunofluorescent staining confirmed reduced Bcrp and Mrp4 and elevated Mrp1 and Mrp5 protein in activated microglia. Pharmacological inhibition of NF-κB transcriptional signaling attenuated down-regulation of Mdr1a mRNA and potentiated up-regulation of Mrp5 mRNA in LPS-treated cells. Together, these data suggest that LPS stimulates microglia and impairs efflux of prototypical ABC transporter substrates by altering mRNA and protein expression, in part through NF-κB signaling. Decreased transporter efflux function in microglia may lead to retention of toxic chemicals and aberrant cell-cell communication during neuroinflammation.

JPET Fast Forward. Published on August 31, 2012 as DOI: 10.1124/jpet.112.196543
This article has not been copyedited and formatted. The final version may differ from this version.

Introduction

ATP-binding cassette (ABC) efflux transporters are a large group of transmembrane proteins responsible for the efflux of endogenous substances and xenobiotics. Although a significant amount of research has focused on the expression and regulation of these transporters in the liver and kidneys (reviewed in Klaassen and Aleksunes, 2010), research has more recently focused on the localization and function of these transporters in the brain (reviewed in Dallas et al., 2006). In the brain, efflux proteins are expressed on brain capillary endothelial cells and are critical in the blood-brain-barrier extrusion of toxic chemicals and drugs from the parenchyma (Elali and Hermann, 2011; Warren et al., 2009). Members from major classes of transporters [multidrug resistance protein 1 (MDR1/ABCB1), multidrug resistance-associated protein 1-5 (MRP1-5/ABCC1-5), and the breast cancer resistance protein (BCRP/ABCG2)] have been found in one or more cell types in the brain, including endothelial cells, neurons, astrocytes, and microglia (reviewed in Klaassen and Aleksunes, 2010).

Microglia are the resident immune cells of the central nervous system and have important responsibilities including neuron support and nutrition as well as immune surveillance. In adult animals, microglia are generally present in a stationary, ramified state and continuously monitor the neural parenchyma through finger-like cytoplasmic projections. Microglia can be stimulated by infections, cerebral ischemia, traumatic brain injury, or neuronal/parenchymal damage to remove necrotic and apoptotic debris and coordinate immune responses (Badoer, 2010; Cao et al., 2011a; Rogers et al., 2007). Activated microglia progressively increase in number during the normal aging process and are also commonly present in neurodegenerative diseases. Activation of microglia is characterized by the production of proinflammatory cytokines as well as

JPET Fast Forward. Published on August 31, 2012 as DOI: 10.1124/jpet.112.196543
This article has not been copyedited and formatted. The final version may differ from this version.

morphological changes, including retraction of cell processes, increased size, and an amoeboid shape (Kim and Joh, 2006). The degree of activation, localization, and types of cytokines produced varies by the type of insult. After resolution of an acute response, some microglia undergo apoptosis while others return to the ramified state (Cao et al., 2011a). However, under certain circumstances, including neurodegenerative diseases, microglia can persist in an activated state (Kim and Joh, 2006; Long-Smith et al., 2009; Vazquez-Claverie et al., 2009; Yasuda et al., 2007). Recently, a role for these transporters in neurodegenerative diseases was postulated since some ABC isoforms can efflux mediators of neuronal injury such as β-amyloid (Hartz et al., 2010). Likewise, the expression of ABC transporters can be modulated by inflammation. For example, the hepatic expression and function of Mdr1a/1b are reduced in rodent models of inflammation using exogenous administration of lipopolysaccharide (LPS) or pro-inflammatory cytokines (Ando et al., 2001; Hartmann et al., 2001).

With recent evidence suggesting that microglia play a prominent role in brain inflammation and neurodegenerative diseases, we hypothesized that ABC transporter function is disrupted in activated microglia, which could alter cell-cell communication and chemical sequestration in the brain. BV-2 cells are immortalized mouse microglia that produce a wide variety of cytokines and other substances, similar to *in vivo* inflammatory responses, making them an ideal tool for mechanistic studies (Cao et al., 2011b; Henn et al., 2009). One signaling pathway implicated in microglial activation is the transcription factor nuclear factor kappa B (NF-κB; Cao et al., 2011b), which has also been shown to regulate expression of efflux transporters (Ronaldson et al., 2010; Yu et al., 2011). Therefore, the purpose of the present study was to 1) quantify ABC transporter function and expression in BV-2 microglia cells, 2) investigate whether transporter

JPET Fast Forward. Published on August 31, 2012 as DOI: 10.1124/jpet.112.196543
This article has not been copyedited and formatted. The final version may differ from this version.

function and expression are altered in response to activation with LPS, and 3) determine whether inhibition of NF-κB signaling alters transporter mRNA regulation in activated microglia.

JPET Fast Forward. Published on August 31, 2012 as DOI: 10.1124/jpet.112.196543
This article has not been copyedited and formatted. The final version may differ from this version.

Materials and Methods

Chemicals. Unless otherwise specified, chemicals were obtained from Sigma-Aldrich (St. Louis, MO).

Cell Culture. The immortalized mouse (C57Bl/6) microglia cell line, BV-2, was used for all experiments (Henn et al., 2009). Cells were grown in modified Eagle's medium (Mediatech, Manassas, VA) supplemented with 10% fetal bovine serum (Atlanta Biologicals, Lawrenceville, GA), 5% sodium pyruvate (Mediatech), 5% non-essential amino acids (Mediatech), and 1% penicillin-streptomycin (Invitrogen, Carlsbad, CA). Cells were incubated at 37°C with 5% CO_2. Cells were used in experiments when they reached 80 to 90% confluence. BV-2 cells were activated with LPS from *E. coli* 026:B6 (Sigma-Aldrich, St. Louis, MO) for up to 24 hours. LPS was dissolved in sterile water at a concentration of 1 mg/ml (stock solution). An equal volume of sterile water was added to all control treatments.

Cell Morphology. Cell morphology was evaluated visually with phase contrast imaging using an inverted microscope (Zeiss Axio Observer, Thornwood, NY). Cell morphology was also characterized in real-time using an xCELLigence RTCA DP analyzer (Roche, Pleasanton, CA). Briefly, BV-2 cells were trypsinized, counted, and seeded evenly (5×10^3 cells) into each well of an E-Plate 16 (Roche). Impedance measurements were recorded every minute during the first two hours of the attachment phase and then every 15 minutes overnight. The next morning, medium was removed and cells were treated with either fresh medium containing vehicle (sterile water) or LPS (100 ng/ml) (0 h time point). Impedance was measured every minute for 100

JPET Fast Forward. Published on August 31, 2012 as DOI: 10.1124/jpet.112.196543
This article has not been copyedited and formatted. The final version may differ from this version.

minutes and then every 15 minutes for 24 hours. Impedance measurements were recorded as a combined cellular index of proliferation, viability, and morphology changes.

Quantitative Transporter Function. Transporter function was quantitated on a Cellometer Vision (Nexcelom Bioscience LLC., Lawrence, MA) cell counter using fluorescent substrates. The technique was adapted from Robey *et al.* (Robey et al., 2011). Briefly, cells were grown in T75 flasks to 80% confluence, trypsinized, and seeded into round bottom wells of a 96-well plate. Cells were then centrifuged at 500 x *g* for 5 minutes at 5°C, resuspended, and loaded with fluorescent substrate with or without inhibitor for 30 minutes at 37°C, 5% CO_2 (*uptake period*). Fluorescent substrate and inhibitor concentrations are provided in Table 1. All transporter substrates and inhibitors were initially dissolved in dimethyl sulfoxide (DMSO). Equal volumes of DMSO were added to all controls when appropriate (final concentration of DMSO was less than 0.5%). Cells were then washed, centrifuged, resuspended, and incubated in substrate-free medium in the presence and absence of inhibitor for 1 hour (*efflux period*). Cells were then washed, resuspended in cold phosphate-buffered saline, and fluorescence quantified using the Nexcelom Vision cellometer. Twenty microliters of cell suspension were applied to the cell counting chamber and each sample was analyzed using the bright-field images for cell size and cell number. The intensity of fluorescence for each cell was subsequently analyzed using filter cubes VB-450-302 (Hoechst 33342; Excitation / Emission: 375nm/450nm), VB-535-402 (Calcein, BODIPY, NBD; Excitation / Emission: 475nm/535nm), or VB-595-502 (Rhodamine 123; Excitation / Emission: 525nm/595nm). The total number of cells analyzed for each sample ranged from 200 to 2000. Raw fluorescence intensity for each cell was normalized to cell size to account for any changes in cell size during microglial activation. The average fluorescence for

JPET Fast Forward. Published on August 31, 2012 as DOI: 10.1124/jpet.112.196543
This article has not been copyedited and formatted. The final version may differ from this version.

each sample was determined and the treatment average was based on 4 independent samples for each treatment.

RNA Isolation and Real-Time Quantitative PCR (qPCR). Cultured BV-2 cells (5 x 10^5 cells/well) were plated onto 6-well tissue culture plates and incubated overnight until attachment. Quadruplicates were treated with vehicle, 1, 10, 100, or 500 ng/ml LPS in fresh medium. After 12 hours of incubation, cell cultures were washed twice with PBS and lysed with Buffer RLT (Qiagen, Valencia, CA) containing 1% β-mercaptoethanol. Total RNA was isolated using the RNeasy mini kit (Qiagen). Complimentary DNA (cDNA) was generated with the First Strand SuperScript cDNA synthesis kit (Invitrogen). cDNA purity and concentration were assessed using a Nanodrop 1000 spectrophotometer (Thermo Scientific, Rockford, IL). For qPCR, specific forward and reverse primers (Integrated DNA Technologies, Coralville, IA) for each gene were added to one microgram of cDNA from each sample. Sybr Green (Applied Biosystems, Carlesbad, CA) was used for detection of amplified products. qPCR was performed in a 384-well plate format using the ABI 7900HT PCR system (Applied Biosystems). Ct values were converted to delta delta Ct values by comparing to a reference gene, ribosomal protein 13a (Rpl13a). Primer sequences for all target mRNAs are provided in Supplemental Table 1.

Western Blot Analysis. BV-2 cells (1 x 10^6 cells) were plated onto 60mm cell culture dishes and allowed to attach overnight. Triplicates were treated with fresh media containing vehicle, 1, 10, 100, or 500 ng/ml LPS and incubated at 37°C for 24 hours. Cells were then washed twice in PBS. Cells were collected, transferred to a microcentrifuge tube, and centrifuged at 1000 x *g* for 10 minutes. The supernatant was removed and the pellet was resuspended in cell lysis buffer

JPET Fast Forward. Published on August 31, 2012 as DOI: 10.1124/jpet.112.196543
This article has not been copyedited and formatted. The final version may differ from this version.

with protease inhibitors. Protein concentration was determined using the bovine serum albumin protein kit (Thermo-Scientific). Western blot analysis of ABC transporters was performed using 50 μg protein homogenate per well by SDS-PAGE on NuPage 8% gels (Invitrogen). Proteins were transferred overnight to a polyvinylidene fluoride membrane. Membranes were blocked in 5% nonfat dry milk in phosphate-buffered saline (PBS) with 0.5% Tween-20. Primary antibodies were diluted in 2% nonfat dry milk and incubated with membranes for 3 hours at the following concentrations: 1:1000 for Mdr1a/b (C219, Novus Biologicals, Littleton, CO), 1:2000 for Mrp1 (MRPr1, Alexis/Enzo Life Sciences, Farmingdale, NY), 1:2000 for Mrp4 (M_4I-80, Alexis/Enzo), 1:500 for Mrp5 (M_5I-10, G. Scheffer, VU Medical Center, Amsterdam, The Netherlands), 1:5000 for Bcrp (BXP-53, Alexis/Enzo), and 1:5000 for Gapdh (Millipore, Temecula, CA). Primary antibodies were probed using species-appropriate secondary antibodies (Sigma) and detected using SuperSignal West Dura blotting reagents (Thermo-Scientific). Detection and semi-quantification of protein bands was performed using a FluorChem imager (Alpha Innotech, San Leandro, CA).

Indirect Immunofluorescent Staining. BV-2 cells (5 x 10^5 cells) were seeded into chambers of a chamber slide (Fisher Scientific) and allowed to attach overnight. The following day, cells were washed twice in PBS. Chambers were either filled with medium alone or medium plus 100 ng/ml LPS and incubated for 24 hours. Slides were fixed with 4% paraformaldehyde, washed twice in PBS, once in PBS with 0.1% triton X-100 and then blocked with 5% goat serum in PBS with 0.1% triton X-100. Slides were then incubated in primary antibody or 5% goat serum, washed, incubated again with the secondary antibody-conjugated to AlexaFluor 488 (Molecular Probes, Eugene, OR), washed, and dried. Slides were coverslipped with Prolong Gold containing

JPET Fast Forward. Published on August 31, 2012 as DOI: 10.1124/jpet.112.196543
This article has not been copyedited and formatted. The final version may differ from this version.

4',6-Diamidino-2-phenylindole (DAPI) (Molecular Probes). Images were acquired on a Zeiss Observer D1 microscope (Zeiss Inc., Thornwood, NY) with an X-Cite series 120Q fluorescent illuminator and a Jenoptik camera with ProgRes CapturePro 2.8 software (Jenoptik, Easthampton, MA). Images were cropped and brightness and contrast were adjusted equally in Adobe Photoshop CS2 (San Jose, CA). All sections were both stained and imaged under uniform conditions for each antibody. Negative controls without primary antibody were included to ensure minimal non-specific staining (data not shown).

NF-κB Inhibition. Cultured BV-2 cells (5 x 10^5 cells/well) were pre-incubated with vehicle (DMSO) or the NF-κB inhibitor (5 μM) InSolution™ BAY 11-7082 (EMD Biosciences, San Diego, CA) for 30 minutes in triplicate. After pre-incubation, cells were treated with vehicle or 100 ng/ml LPS in the absence or presence of BAY 11-7082. After 12 hours of incubation, cell culture medium was removed and frozen for quantification of tumor necrosis factor α (TNFα) protein. Cell cultures were washed and lysed. RNA isolation, cDNA synthesis, and qPCR were performed as described above.

TNFα Protein Quantification. TNFα levels were quantified in cell culture medium using a mouse ELISA kit (Invitrogen) according to the manufacturer's instructions.

Statistical Analysis. GraphPad Prism© version 5 software (GraphPad Software, La Jolla, CA) was used for statistical analysis. Differences among groups were determined by either a two-tailed t test when only two groups were compared, or a one-way analysis of variance with a Newman-Keul's posthoc test for multiple group comparisons. Differences were considered statistically significant at $p < 0.05$.

JPET Fast Forward. Published on August 31, 2012 as DOI: 10.1124/jpet.112.196543
This article has not been copyedited and formatted. The final version may differ from this version.

Results

Basal expression and function of ABC efflux transporters in BV-2 cells. Resting BV-2 microglia express ABC transporter mRNA including Mrp1-5, Mdr1a, Mdr1b, and Bcrp. Messenger RNA expression in BV-2 cells was compared to mouse liver after normalizing to the reference gene Rpl13a (Table 2). The expression of transporter mRNA differed between BV-2 microglia and mouse liver. After normalizing to Rpl13a, BV-2 microglia had negligible amounts of Mrp2 mRNA compared to mouse liver. BV-2 cells also expressed lower levels of Mrp3 and Bcrp mRNA. In contrast, microglia expressed high levels of Mrp1, Mrp4, Mrp5, Mdr1a, and Mdr1b mRNA compared to mouse liver. Basal transporter function was quantified in control BV-2 cells using a fluorescent cell counter (Fig. 1) as described by Robey *et al.* (Robey et al., 2011). A panel of fluorescent chemicals (rhodamine, calcein AM, and Hoechst 33342) and inhibitors against various ABC transporters were tested (Table 1). Inhibition of Mdr1 with PSC833 significantly increased accumulation of rhodamine 123 in BV-2 cells by 84%. Compared to control cells, MK-571, a general inhibitor of Mrps, significantly enhanced calcein AM fluorescence by 108%. The Bcrp inhibitor KO143 significantly increased Hoechst 33342 levels by 51% (Fig 1A). Images demonstrating fluorescent dye retention in BV-2 cells in the presence of prototypical inhibitors are shown in Fig. 1B.

Lipopolysaccharide activation of BV-2 microglia. Altered BV-2 cell morphology in response to LPS was assessed quantitatively by changes in impedance using real-time measurements (Fig. 2A) and qualitatively by light microscopy (Supplemental Fig. 1). Greater electrical impedances across interdigitating microelectrodes on the bottom of the culture plate reflect collective changes in cell morphology, viability, and proliferation. As cells occupy a larger surface area on

the electrodes, the path that a small electrical current must travel through the cell membrane is longer which results in increased electrical impedance. In the present study, the early attachment and longer growth phases of plated BV-2 cells were clearly observed with slow, gradual increases in impedance over 24 hours (Time = -24 to 0 hours). Upon addition of 100 ng/ml LPS (Time = 0 hours), an immediate and dramatic change in the impedance was detected in LPS-treated cells (*blue*) as compared to control cells (*red*). The peak of the impedance difference between control and LPS-treated cells occurred 4 hours after addition of LPS. Morphological changes were confirmed at 6 hours with phase contrast microscopy (Supplemental Figs. 1A and B). BV-2 cells without exposure to LPS were 10 to 15 μm in diameter, uniformly round, with occasional thin cytoplasmic projections. After LPS activation, BV-2 cells were much larger in diameter (25 to 30 μm), polymorphic, with many exhibiting thick cytoplasmic projections. Compared to vehicle-treated cells, incubation with 100 ng/ml LPS for 24 hours did not alter cell number or cell viability as determined by the alamar Blue assay (data not shown). These data suggest that the quantitative differences in cell impedance were largely due to the observed morphologic changes. By 20 hours, cell impedance values were similar between control- and LPS-treated cells. In addition to morphologic changes, activated microglia produced pro-inflammatory cytokines including TNFα, interleukin-1β (IL-1β), and interleukin-6 (IL-6). Messenger RNA levels of TNFα, IL-1β, and IL-6 were dose-dependently increased in BV-2 cells in response to LPS at 12 hours (Fig. 2B). Stimulation of TNFα cytokine mRNA expression was achieved even at the lowest concentration of LPS (1 ng/ml).

Activation of microglia decreases efflux transporter function and increases intracellular retention of substrates. Activation of BV-2 microglia with 100 ng/ml LPS for 24 hours

JPET Fast Forward. Published on August 31, 2012 as DOI: 10.1124/jpet.112.196543
This article has not been copyedited and formatted. The final version may differ from this version.

enhanced intracellular accumulation of all fluorescent substrates tested (Figs. 3A and 3B). Retention of rhodamine 123, an Mdr1 substrate, was increased approximately 25% in LPS-activated microglia (Fig. 3A). The distribution curve shows a larger percentage of cells had more fluorescence indicated by a right shift in the curve. Retention of calcein AM, an Mrp substrate, increased 110% in LPS-treated microglia. Most control BV-2 cells had minimal calcein AM fluorescence suggesting efficient efflux during the 1 hour incubation period. In contrast, the majority of activated microglia exhibited strong retention of calcein AM, indicated by a right shift in the distribution of cellular fluorescence. Hoechst 33342, a Bcrp substrate, also shows greater average fluorescence and retention in activated microglia, although at a much lower degree than the other efflux transporters. Two additional chemicals including a pharmaceutical and an endogenous signaling molecule were included as examples of relevant ABC efflux substrates. Efflux of the α-adrenergic antagonist, prazosin, and the pro-apoptotic molecule, ceramide, was also inhibited by LPS treatment (Fig. 3B). Mean fluorescence for prazosin and ceramide increased 39% and 90%, respectively, after microglial activation with LPS. Images demonstrating fluorescent dye retention in control- and LPS-treated BV-2 cells are shown in Supplemental Fig. 2. Cellular loading and uptake of all substrates tested was not altered by LPS treatment (Supplemental Fig. 3), demonstrating that changes in cellular retention of substrates in response to LPS are due to differences in chemical efflux rather than uptake.

Decreased efflux transporter function is paralleled by down-regulation of transporter mRNA. Messenger RNA expression of ABC transporters was quantified after microglial activation with LPS treatment (Fig. 4). Transporter mRNA expression of most efflux transporters decreased by 12 hours after initiation of LPS treatment. Mrp2 and Mrp3 mRNA decreased 60%

JPET Fast Forward. Published on August 31, 2012 as DOI: 10.1124/jpet.112.196543
This article has not been copyedited and formatted. The final version may differ from this version.

at the lowest concentration (1 ng/ml LPS) with no further declines observed at higher LPS concentrations. All other efflux transporters exhibited concentration-dependent changes with increasing LPS concentrations. In BV-2 cells treated with 500 ng/ml LPS, levels of Mrp1 and Mrp5 mRNA rose by 150% and 300%, respectively, whereas Mdr1a, Mdr1b, and Bcrp mRNAs were reduced by 70%, 75%, and 55%, respectively.

Transporter protein expression is consistent with altered function and mRNA levels. Western blot analysis of transporter proteins showed high basal protein expression of Mdr1, Bcrp, Mrp1, and Mrp4 in cultured BV-2 microglia (Fig. 5). Mouse liver, kidney, and placenta homogenates were used as positive controls for each transporter (data not shown). Mrp5 basal protein expression was relatively low. Upon LPS stimulation of BV-2 microglia for 24 hours, Mrp4, Mdr1, and Bcrp proteins were significantly decreased by up to 55%, 42%, and 42%, respectively. Mrp1 and Mrp5 proteins were elevated up to 140% and 210%, respectively, after LPS treatment. Protein expression for all transporters followed the same pattern as their respective mRNAs. Notably, Mrp2 and Mrp3 proteins were neither present in control cells nor induced by LPS (data not shown). Qualitative transporter expression was assessed in paraformaldehyde-fixed BV-2 cells using specific transporter antibodies (Fig. 6). Treatment of BV-2 cells with 100 ng/ml LPS for 24 hours intensified the diffuse and plasma membrane staining of Mrp1 and Mrp5 proteins and resulted in multiple intensely fluorescent foci. Decreased staining of Mrp4 and Bcrp proteins was observed in LPS-treated cells. There are no commercial antibodies capable of selectively staining Mdr1 protein in cells of mouse origin.

JPET Fast Forward. Published on August 31, 2012 as DOI: 10.1124/jpet.112.196543
This article has not been copyedited and formatted. The final version may differ from this version.

Inhibition of NF-κB attenuates LPS-induced Mdr1a down-regulation and potentiates Mrp5 up-regulation. LPS activation of the toll-like receptor-4 results in downstream NF-κB activation through phosphorylation of IκB, the inhibitory protein of NF-κB. NF-κB is then free to enter the nucleus where it increases the mRNA transcription of several genes including TNFα, IL-1β, and IL-6. BAY 11-7082 inhibits the phosphorylation of IκB, resulting in the stabilization of the IκB/NF-κB complex and inhibition of NF-κB-mediated transcription (Min et al., 2011). Compared to LPS alone, co-treatment of BV-2 cells with LPS and BAY 11-7082 attenuated IL-1β and IL-6 cytokine mRNA induction by approximately 75% (Fig. 7A and B). Surprisingly, TNFα mRNA was increased further by co-treatment of cells with LPS and BAY 11-7082 (Fig 7C). However, secreted TNFα protein in the cell culture media of BAY 11-7082 treated cells was decreased by approximately 75%, confirming inactivation of NF-κB signaling (Fig. 7D).

Inhibition of NF-κB with BAY 11-7082 attenuated the decrease in Mdr1a mRNA that resulted from LPS activation of microglia (Fig 8). Treatment with BAY 11-7082 did not affect the LPS-induced down-regulation of Bcrp or Mdr1b mRNA. BAY 11-7082 also caused an increase in Mrp5 mRNA in control cells and potentiated the increase of Mrp5 in LPS-treated cells (Fig. 9). Although not statistically significant, Mrp1 mRNA showed a similar trend to Mrp5 using BAY 11-7082. In order to further investigate the enhancement of Mrp5 mRNA by BAY 11-7082, the mRNA expression of the oxidative stress transcription factor nuclear factor e2-related factor 2 (Nrf2) and its target genes NAD(P)H quinone oxidoreductase 1 (Nqo1) and heme oxygenase-1 were quantified. This signaling pathway has been previously shown to regulate expression of some Mrps (Maher et al., 2007). Interestingly, BAY 11-7082 increased Nrf2 mRNA in LPS-

treated cells and elevated mRNA levels of Nqo1 (Fig 9) and heme oxygenase-1 (data not shown) in control- and LPS-treated cells.

JPET Fast Forward. Published on August 31, 2012 as DOI: 10.1124/jpet.112.196543
This article has not been copyedited and formatted. The final version may differ from this version.

Discussion

The present study investigated the regulation of ABC efflux transporter function in activated microglia. Significant reductions in the cellular accumulation of fluorescent substrates after a 60-minute efflux period demonstrated basal activity of Mrps, Mdr1, and Bcrp in BV-2 cells. On the other hand, LPS-treated microglia had greater intracellular fluorescence, which suggested that microglial activation decreased the function of efflux transporters. The retention of fluorescent substrates was similar to, and in some cases greater than, the retention observed with known transporter inhibitors. These data indicate that efficient efflux of chemicals in resting microglia is impaired during microglial activation and neuroinflammation.

BV-2 cells as a model for microglial activation. In this study, we confirmed the presence of ABC efflux transporters in BV-2 cells and showed that they are similar to primary microglia and *in vivo* rodent studies. Several groups have shown that cultured rat primary microglia and the rat MLS-9 microglia cell line express functional Mrp1, 4, 5, and Mdr1 proteins but are deficient in Mrp2 protein (Ballerini et al., 2002; Dallas et al., 2003; 2004; Hirrlinger et al., 2002; Lee et al., 2001). Initial studies in our laboratory comparing BV-2 cells with primary microglia from neonatal C57BL/6 mice have shown similar mRNA for most efflux transporters including Mrp1, Mrp2, and Mrp5. Mdr1a/1b mRNAs were up to 50% less abundant in primary microglia (data not shown). Notably, mRNA quantities were approximately 7-fold lower and 10-fold higher in primary microglia for Mrp4 and Bcrp, respectively. From a functional aspect, the MLS-9 cell line has been shown to lack Bcrp-mediated efflux of mitoxantrone (Lee et al., 2007). This is similar to our data demonstrating modest differences in Bcrp-mediated Hoechst 33342 retention in BV-2 cells under various experimental conditions. Additionally, Dauchy *et al.* (2008)

JPET Fast Forward. Published on August 31, 2012 as DOI: 10.1124/jpet.112.196543
This article has not been copyedited and formatted. The final version may differ from this version.

determined that MRP2 and MRP3 mRNA are not present in human cortex or isolated microvessels and concluded that BCRP and MDR1 represent the primary ABC transporters in human microvessels with relatively low amounts of MRP1, 4, and 5 (Dauchy et al., 2008). Human cerebral cortex samples, on the other hand, had greater expression of MRP5, BCRP, and MRP1 mRNA, suggesting that other cell types including microglia express a unique set of efflux transporters (Dauchy et al., 2008; Warren et al., 2009).

Transporter protein response to inflammation. Although transporters function similarly to export substrates from cells, they are likely regulated by different mechanisms. This is supported by the fact that Mrp1 and Mrp5 mRNA and protein were up-regulated by LPS whereas all other transporters were decreased. The reduced function of Mrp1 (calcein AM retention), despite the up-regulation of mRNA and protein, may be due to altered membrane trafficking, loss of a transport co-substrate, or a compensatory response. The multiple foci of Mrp1 staining in LPS-treated cells suggest that trafficking to the plasma membrane may be altered despite an increase in total protein. Alternatively, functional inhibition of Mrp1 may result from the depletion of glutathione, which is a transport co-substrate. Resting microglia have high amounts of glutathione which is rapidly oxidized in activated microglia that are producing reactive oxygen species (Hirrlinger et al., 2000; Rudd et al., 2011). Glutathione depletion could lead to decreased function of Mrp1. It is also conceivable that up-regulation of Mrp1 may be a compensatory response to impaired function.

Inflammation causes similar changes in transporter expression in the liver. Mrp1 and Mrp5 mRNA in livers of mice exposed to LPS are up-regulated, similar to activated BV-2 microglia

(Lickteig et al., 2007). LPS also decreases the function, mRNA, and protein expression of Mdr1 in rodent livers (Fernandez et al., 2004; Piquette-Miller et al., 1998). Additional studies point to IL-6 and/or TNFα as key cytokines responsible for hepatic Mdr1 down-regulation in rodents during inflammation (Ando et al., 2001; Hartmann et al., 2001). Regulation of Mdr1 expression in the brain by LPS is less consistent; however, there appears to be a uniform decline in function in human cell culture models and rodent studies regardless of expression levels (Fernandez et al., 2004; Goralski et al., 2003; Hartz et al., 2006).

Initial studies conducted in primary microglia isolated from neonatal C57BL/6 mice demonstrate transporter mRNA changes after LPS activation that are similar to BV-2 cells (data not shown). Treatment of primary microglia with LPS increased Mrp1 mRNA and decreased Bcrp mRNA at 12 hours. Additional dose- and time-course responses of primary microglia are needed to further investigate the regulation of transporter expression as well as function during neuroinflammation.

Transcription factor signaling. Few studies have investigated the signaling mechanisms underlying regulation of Mdr1 and other transporters in response to LPS (Morgan et al., 2008; Teng and Piquette-Miller, 2008). In the present study, inhibition of the NF-κB transcription factor pathway, which regulates cytokine production, attenuated Mdr1a mRNA down-regulation. Evidence of impaired NF-κB signaling by BAY 11-7082 was observed in TNFα protein and IL-6 and IL-1ß mRNA. Somewhat paradoxically, TNFα mRNA was induced in co-treated cells, possibly through alternate pathways to compensate for lower protein levels.

JPET Fast Forward. Published on August 31, 2012 as DOI: 10.1124/jpet.112.196543
This article has not been copyedited and formatted. The final version may differ from this version.

In contrast to Mdr1, Mrp1 was not affected by inhibition of NF-κB. In primary rat astrocytes, Ronaldson *et. al*. (2010) found that expression of Mrp1 protein and transport increased after treatment with TNFα. This finding is in contrast to the functional decrease of Mrp1 in microglial cells. This discrepancy may be related to the inherently different functional responses of astrocytes and microglia to TNFα and LPS, respectively. From a mechanistic standpoint, inhibition of NF-κB did not prevent Mrp1 expression changes in astrocytes treated with TNFα (Ronaldson et al., 2010). Similarly, we found that inhibiting NF-κB in LPS-treated microglia did not interfere with Mrp1 induction, indicating that Mrp1 mRNA is not directly regulated by NF-κB.

Nrf2 regulates the expression of Mrp1 in cultured mouse fibroblasts (Hayashi et al., 2003). Likewise, pharmacological activation of Nrf2 increases Mrp5 mRNA in mouse liver (Maher et al., 2005). In the present study, mRNA expression of the Nrf2 target, Nqo1, was up-regulated by LPS and BAY 11-7082 supporting Nrf2 activation as a candidate transcriptional pathway for Mrp1 and Mrp5 up-regulation. Nrf2 activation is likely a result of NF-κB signaling, cytokine production, and oxidative stress associated with microglial activation. Nrf2 dampens LPS-induced microglial activation and lowers the production of pro-inflammatory cytokines in BV-2 cells (Koh et al., 2009; 2011; Lee et al., 2011). Interestingly, inhibition of NF-κB in microglia using BAY 11-7082 resulted in the up-regulation of Nqo1 rather than down-regulation as would be expected if there was direct cross-talk between NF-κB and Nrf2. One possible explanation is that BAY 11-7082 also acts independent of NF-κB to activate Nrf2. In fact, BAY 11-7082 has been shown to increase mRNA and protein of Nrf2 responsive genes in a Nrf2-dependent

JPET Fast Forward. Published on August 31, 2012 as DOI: 10.1124/jpet.112.196543
This article has not been copyedited and formatted. The final version may differ from this version.

manner in human colorectal cells likely through production of reactive oxygen species (Min et al., 2011).

Implications of altered ABC transport function in neuroinflammation. Our study provides novel information regarding efflux processes in activated microglia that may alter signaling with other neuronal cells. Activation of microglia was initially believed to be a response to neurodegeneration. However, it is now widely accepted that microglia play a more active or even primary role in initiating neuronal injury (Cao et al., 2011a; Kim and Joh, 2006; Long-Smith et al., 2009; Rogers et al., 2007; Ros-Bernal et al., 2011; Yokoyama et al., 2011). Activated microglia have been detected in living and postmortem Parkinson's disease patients (Gerhard et al., 2006; McGeer et al., 1988; Mirza et al., 2000) and in samples from humans and monkeys with 1-methyl-4-phenyl-1,2,3,6-tetrahydropyridine-induced Parkinson's disease (Langston et al., 1999; McGeer et al., 2003). Activated microglia are implicated in direct neuronal degeneration (Block et al., 2007). Amyloid beta, lipid peroxides, prostaglandins, pesticides, and other chemicals have been found to either influence the expression of, or are themselves substrates for, efflux transporters (Kania et al., 2011; Oosterhuis et al., 2008; Rudd et al., 2011; Sreeramulu et al., 2007; Yang et al., 2011). The pro-apoptotic protein ceramide was also markedly retained in LPS-activated microglia in the present study. Collectively, these findings suggest the potential ability of transporters to regulate the accumulation of potentially detrimental compounds within the brain.

The active role of neuroinflammation and microglial activation in neurodegenerative disease has led to several studies examining the relationship of anti-inflammatory drug use and risk of

neurodegeneration. Human epidemiologic studies have shown an inverse association between non-steroidal anti-inflammatory drugs (NSAIDs) use and the risk of developing Parkinson's disease (McGeer and McGeer, 1998; Chen et al., 2005). Likewise, the incidence of Alzheimer's disease may be delayed by NSAID use in asymptomatic patients (Breitner et al., 2011). Although the benefit of NSAIDs in these patient populations is likely related to the general suppression of inflammation, modulation of transporter expression in microglia may aid in restoring normal cell-cell communication. Studies examining drug transporters using non-steroidal anti-inflammatory drugs (NSAIDs) have yielded conflicting results depending on the model system used and the type of NSAID. Jung et. al. showed that aspirin induces MDR1 mRNA and activity in intestinal cells *in vitro* and rat intestine *in vivo* (Jung et al., 2011). In another study, NSAIDs increased MDR1 mRNA expression in Caco-2 cells but not efflux activity (Takara et al., 2009). Thus, the use of NSAIDs to attenuate neuroinflammation and microglial activation may have the added benefit of partially restoring normal transporter function.

Conclusions

We have demonstrated that activation of microglia with LPS alters chemical transport by differentially regulating the expression of ABC transporters. Understanding how microglia communicate, react, and interact with the neuronal environment, particularly through the expression of transporters, may help in determining mechanisms of neurodegeneration and development of possible interventions. Future studies should aim to verify altered ABC transporter expression and function in animal models of neuroinflammation and neurological disease.

Acknowledgements

The authors appreciate the use of the xCELLigence RTCA DP analyzer by Roche Diagnostics (Pleasanton, CA) for real-time impedance measurements. The authors are grateful for BV-2 cells provided by Dr. Bin Liu, University of Florida, antibodies provided by Dr. George Scheffer, VU Medical Center, Amsterdam, The Netherlands and qPCR primers from Dr. Angela Slitt, University of Rhode Island, RI.

Authorship Contributions

Participated in research design: Gibson, Richardson, Aleksunes

Conducted experiments: Gibson, Hossain

Contributed new reagents or analytic tools: Richardson, Aleksunes

Performed data analysis: Gibson

Wrote or contributed to the writing of the manuscript: Gibson, Richardson, Aleksunes

References

Ando H, Nishio Y, Ito K, Nakao A, Wang L, Zhao YL, Kitaichi K, Takagi K, Hasegawa T. (2001) Effect of endotoxin on P-glycoprotein-mediated biliary and renal excretion of rhodamine-123 in rats. *Antimicrob Agents Chemother* **45**:3462-3467.

Badoer E. (2010) Microglia: Activation in acute and chronic inflammatory states and in response to cardiovascular dysfunction. *Int J Biochem Cell Biol* **42**:1580-1585.

Ballerini P, Di Iorio P, Ciccarelli R, Nargi E, D'Alimonte I, Traversa U, Rathbone MP, Caciagli F. (2002) Glial cells express multiple ATP binding cassette proteins which are involved in ATP release. *Neuroreport* **13**:1789-1792.

Block ML, Zecca L, Hong JS. (2007) Microglia-mediated neurotoxicity: Uncovering the molecular mechanisms. *Nat Rev Neurosci* **8**:57-69.

Breitner JC, Baker LD, Montine TJ, Meinert CL, Lyketsos CG, Ashe KH, Brandt J, Craft S, Evans DE, Green RC, Ismail MS, Martin BK, Mullan MJ, Sabbagh M, Tariot PN. (2011) Extended results of the Alzheimer's disease anti-inflammatory prevention trial. *Alzheimers Dement* **7**:402-11.

Cao JJ, Li KS, Shen YQ. (2011a) Activated immune cells in parkinson's disease. *J Neuroimmune Pharmacol* **6**:323-329.

Cao Q, Kaur C, Wu CY, Lu J, Ling EA. (2011b) Nuclear factor-kappa beta regulates notch signaling in production of proinflammatory cytokines and nitric oxide in murine BV-2 microglial cells. *Neuroscience* **192**:140-154.

Chen H, Jacobs E, Schwarzschild MA, McCullough ML, Calle EE, Thun MJ, Ascherio A. (2005) Nonsteroidal antiinflammatory drug use and the risk for parkinson's disease. *Ann Neurol* **58**:963-967.

Dallas S, Miller D, Bendayan R. (2006) Multidrug resistance-associated proteins: expression and function in the central nervous system. *Pharmacol Rev* **58**: 140-61.

Dallas S, Schlichter L, Bendayan R. (2004) Multidrug resistance protein (MRP) 4- and MRP 5-mediated efflux of 9-(2-phosphonylmethoxyethyl)adenine by microglia. *J Pharmacol Exp Ther* **309**:1221-1229.

Dallas S, Zhu X, Baruchel S, Schlichter L, Bendayan R. (2003) Functional expression of the multidrug resistance protein 1 in microglia. *J Pharmacol Exp Ther* **307**:282-290.

Dauchy S, Dutheil F, Weaver RJ, Chassoux F, Daumas-Duport C, Couraud PO, Scherrmann JM, De Waziers I, Decleves X. (2008) ABC transporters, cytochromes P450 and their main transcription factors: Expression at the human blood-brain barrier. *J Neurochem* **107**:1518-1528.

Elali A and Hermann DM. (2011) ATP-binding cassette transporters and their roles in protecting the brain. *Neuroscientist* **17**:423-436.

Fernandez C, Buyse M, German-Fattal M, Gimenez F. (2004) Influence of the pro-inflammatory cytokines on P-glycoprotein expression and functionality. *J Pharm Pharm Sci* **7**:359-371.

Gerhard A, Pavese N, Hotton G, Turkheimer F, Es M, Hammers A, Eggert K, Oertel W, Banati RB, Brooks DJ. (2006) In vivo imaging of microglial activation with [11C](R)-PK11195 PET in idiopathic parkinson's disease. *Neurobiol Dis* **21**:404-412.

Goralski KB, Hartmann G, Piquette-Miller M, Renton KW. (2003) Downregulation of mdr1a expression in the brain and liver during CNS inflammation alters the in vivo disposition of digoxin. *Br J Pharmacol* **139**:35-48.

Hartmann G, Kim H, Piquette-Miller M. (2001) Regulation of the hepatic multidrug resistance gene expression by endotoxin and inflammatory cytokines in mice. *Int Immunopharmacol* **1**:189-199.

Hartz AM, Bauer B, Fricker G, Miller DS. (2006) Rapid modulation of P-glycoprotein-mediated transport at the blood-brain barrier by tumor necrosis factor-alpha and lipopolysaccharide. *Mol Pharmacol* **69**:462-470.

Hartz AM, Miller DS, Bauer B. (2010) Restoring blood-brain barrier P-glycoprotein reduces brain amyloid-beta in a mouse model of alzheimer's disease. *Mol Pharmacol* **77**:715-723.

Hayashi A, Suzuki H, Itoh K, Yamamoto M, Sugiyama Y. (2003) Transcription factor Nrf2 is required for the constitutive and inducible expression of multidrug resistance-associated protein 1 in mouse embryo fibroblasts. *Biochem Biophys Res Commun* **310**:824-829.

Henn A, Lund S, Hedtjarn M, Schrattenholz A, Porzgen P, Leist M. (2009) The suitability of BV2 cells as alternative model system for primary microglia cultures or for animal experiments examining brain inflammation. *ALTEX* **26**:83-94.

Hirrlinger J, Gutterer JM, Kussmaul L, Hamprecht B, Dringen R. (2000) Microglial cells in culture express a prominent glutathione system for the defense against reactive oxygen species. *Dev Neurosci* **22**:384-392.

Hirrlinger J, Konig J, Dringen R. (2002) Expression of mRNAs of multidrug resistance proteins (mrps) in cultured rat astrocytes, oligodendrocytes, microglial cells and neurones. *J Neurochem* **82**:716-719.

Jung KH, Chu K, Lee ST, Yoon HJ, Chang JY, Nam WS, Yoon SH, Cho JY, Yu KS, Jang IJ, Kim M, Lee SK, Roh JK. (2011) Prolonged use of aspirin alters human and rat intestinal cells and thereby limits the absorption of clopidogrel. *Clin Pharmacol Ther* **90**:612-619.

Kania KD, Wijesuriya HC, Hladky SB, Barrand MA. (2011) Beta amyloid effects on expression of multidrug efflux transporters in brain endothelial cells. *Brain Res* **1418**:1-11.

Kim YS and Joh TH. (2006) Microglia, major player in the brain inflammation: Their roles in the pathogenesis of parkinson's disease. *Exp Mol Med* **38**:333-347.

Klaassen CD and Aleksunes LM. (2010) Xenobiotic, bile acid, and cholesterol transporters: Function and regulation. *Pharmacol Rev* **62**:1-96.

Koh K, Cha Y, Kim S, Kim J. (2009) tBHQ inhibits LPS-induced microglial activation via Nrf2-mediated suppression of p38 phosphorylation. *Biochem Biophys Res Commun* **380**:449-453.

Koh K, Kim J, Jang YJ, Yoon K, Cha Y, Lee HJ, Kim J. (2011) Transcription factor Nrf2 suppresses LPS-induced hyperactivation of BV-2 microglial cells. *J Neuroimmunol* **233**:160-167.

Langston JW, Forno LS, Tetrud J, Reeves AG, Kaplan JA, Karluk D. (1999) Evidence of active nerve cell degeneration in the substantia nigra of humans years after 1-methyl-4-phenyl-1,2,3,6-tetrahydropyridine exposure. *Ann Neurol* **46**:598-605.

Lee G, Babakhanian K, Ramaswamy M, Prat A, Wosik K, Bendayan R. (2007) Expression of the ATP-binding cassette membrane transporter, ABCG2, in human and rodent brain microvessel endothelial and glial cell culture systems. *Pharm Res* **24**:1262-1274.

Lee G, Schlichter L, Bendayan M, Bendayan R. (2001) Functional expression of P-glycoprotein in rat brain microglia. *J Pharmacol Exp Ther* **299**:204-212.

Lee IS, Ryu DK, Lim J, Cho S, Kang BY, Choi HJ. (2011) Artesunate activates Nrf2 pathway-driven anti-inflammatory potential through ERK signaling in microglial BV2 cells. *Neurosci Lett.*

Lickteig AJ, Slitt AL, Arkan MC, Karin M, Cherrington NJ. (2007) Differential regulation of hepatic transporters in the absence of tumor necrosis factor-alpha, interleukin-1beta, interleukin-6, and nuclear factor-kappaB in two models of cholestasis. *Drug Metab Dispos* **35**:402-409.

Long-Smith CM, Sullivan AM, Nolan YM. (2009) The influence of microglia on the pathogenesis of parkinson's disease. *Prog Neurobiol* **89**:277-287.

Maher JM, Cheng X, Slitt AL, Dieter MZ, Klaassen CD. (2005) Induction of the multidrug resistance-associated protein family of transporters by chemical activators of receptor-mediated pathways in mouse liver. *Drug Metab Dispos* **33**:956-962.

Maher JM, Dieter MZ, Aleksunes LM, Slitt AL, Guo G, Tanaka Y, Scheffer GL, Chan JY, Manautou JE, Chen Y, Dalton TP, Yamamoto M, Klaassen CD. (2007) Oxidative and electrophilic stress induces multidrug resistance-associated protein transporters via the nuclear factor-E2-related factor-2 transcriptional pathway. *Hepatology* **46**:1597-1610.

McGeer PL, Itagaki S, Boyes BE, McGeer EG. (1988) Reactive microglia are positive for HLA-DR in the substantia nigra of parkinson's and alzheimer's disease brains. *Neurology* **38**:1285-1291.

McGeer EG and McGeer PL. (1998) The importance of inflammatory mechanisms in alzheimer disease. *Exp Gerontol* **33**:371-378.

McGeer PL, Schwab C, Parent A, Doudet D. (2003) Presence of reactive microglia in monkey substantia nigra years after 1-methyl-4-phenyl-1,2,3,6-tetrahydropyridine administration. *Ann Neurol* **54**:599-604.

Min KJ, Lee JT, Joe EH, Kwon TK. (2011) An IkappaBalpha phosphorylation inhibitor induces heme oxygenase-1(HO-1) expression through the activation of reactive oxygen species (ROS)-Nrf2-ARE signaling and ROS-PI3K/Akt signaling in an NF-kappaB-independent mechanism. *Cell Signal* **23**:1505-1513.

Mirza B, Hadberg H, Thomsen P, Moos T. (2000) The absence of reactive astrocytosis is indicative of a unique inflammatory process in parkinson's disease. *Neuroscience* **95**:425-432.

Morgan ET, Goralski KB, Piquette-Miller M, Renton KW, Robertson GR, Chaluvadi MR, Charles KA, Clarke SJ, Kacevska M, Liddle C, Richardson TA, Sharma R, Sinal CJ. (2008)

Regulation of drug-metabolizing enzymes and transporters in infection, inflammation, and cancer. *Drug Metab Dispos* **36**:205-216.

Oosterhuis B, Vukman K, Vagi E, Glavinas H, Jablonkai I, Krajcsi P. (2008) Specific interactions of chloroacetanilide herbicides with human ABC transporter proteins. *Toxicology* **248**:45-51.

Piquette-Miller M, Pak A, Kim H, Anari R, Shahzamani A. (1998) Decreased expression and activity of P-glycoprotein in rat liver during acute inflammation. *Pharm Res* **15**:706-711.

Robey RW, Lin B, Qiu J, Chan LL, Bates SE. (2011) Rapid detection of ABC transporter interaction: Potential utility in pharmacology. *J Pharmacol Toxicol Methods* **63**:217-222.

Rogers J, Mastroeni D, Leonard B, Joyce J, Grover A. (2007) Neuroinflammation in alzheimer's disease and parkinson's disease: Are microglia pathogenic in either disorder? *Int Rev Neurobiol* **82**:235-246.

Ronaldson PT, Ashraf T, Bendayan R. (2010) Regulation of multidrug resistance protein 1 by tumor necrosis factor alpha in cultured glial cells: Involvement of nuclear factor-kappaB and c-jun N-terminal kinase signaling pathways. *Mol Pharmacol* **77**:644-659.

Ros-Bernal F, Hunot S, Herrero MT, Parnadeau S, Corvol JC, Lu L, Alvarez-Fischer D, Carrillo-de Sauvage MA, Saurini F, Coussieu C, Kinugawa K, Prigent A, Hoglinger G, Hamon M,

Tronche F, Hirsch EC, Vyas S. (2011) Microglial glucocorticoid receptors play a pivotal role in regulating dopaminergic neurodegeneration in parkinsonism. *Proc Natl Acad Sci U S A* **108**:6632-6637.

Rudd LP, Kabler SL, Morrow CS, Townsend AJ. (2011) Enhanced glutathione depletion, protein adduct formation, and cytotoxicity following exposure to 4-hydroxy-2-nonenal (HNE) in cells expressing human multidrug resistance protein-1 (MRP1) together with human glutathione S-transferase-M1 (GSTM1). *Chem Biol Interact* **194**:113-119.

Sreeramulu K, Liu R, Sharom FJ. (2007) Interaction of insecticides with mammalian P-glycoprotein and their effect on its transport function. *Biochim Biophys Acta* **1768**:1750-1757.

Takara K, Hayashi R, Kokufu M, Yamamoto K, Kitada N, Ohnishi N, Yokoyama T. (2009) Effects of nonsteroidal anti-inflammatory drugs on the expression and function of P-glycoprotein/MDR1 in caco-2 cells. *Drug Chem Toxicol* **32**:332-337.

Teng S and Piquette-Miller M. (2008) Regulation of transporters by nuclear hormone receptors: Implications during inflammation. *Mol Pharm* **5**:67-76.

Vazquez-Claverie M, Garrido-Gil P, San Sebastian W, Izal-Azcarate A, Belzunegui S, Marcilla I, Lopez B, Luquin MR. (2009) Acute and chronic 1-methyl-4-phenyl-1,2,3,6-tetrahydropyridine administrations elicit similar microglial activation in the substantia nigra of monkeys. *J Neuropathol Exp Neurol* **68**:977-984.

Warren MS, Zerangue N, Woodford K, Roberts LM, Tate EH, Feng B, Li C, Feuerstein TJ, Gibbs J, Smith B, de Morais SM, Dower WJ, Koller KJ. (2009) Comparative gene expression profiles of ABC transporters in brain microvessel endothelial cells and brain in five species including human. *Pharmacol Res* **59**:404-413.

Yang CN, Shiao YJ, Shie FS, Guo BS, Chen PH, Cho CY, Chen YJ, Huang FL, Tsay HJ. (2011) Mechanism mediating oligomeric abeta clearance by naive primary microglia. *Neurobiol Dis* **42**:221-230.

Yasuda Y, Shinagawa R, Yamada M, Mori T, Tateishi N, Fujita S. (2007) Long-lasting reactive changes observed in microglia in the striatal and substantia nigral of mice after 1-methyl-4-phenyl-1,2,3,6-tetrahydropyridine. *Brain Res* **1138**:196-202.

Yokoyama H, Uchida H, Kuroiwa H, Kasahara J, Araki T. (2011) Role of glial cells in neurotoxin-induced animal models of parkinson's disease. *Neurol Sci* **32**:1-7.

Yu N, Di Q, Liu H, Hu Y, Jiang Y, Yan YK, Zhang YF, Zhang YD. (2011) Nuclear factor-kappa B activity regulates brain expression of P-glycoprotein in the kainic acid-induced seizure rats. *Mediators Inflamm* **2011**:670613.

Footnotes

This work was supported in part by the National Institutes of Health Institute of Diabetes and Digestive and Kidney Diseases [Grants DK080774], the National Institutes of Health Environmental Health Sciences [Grants ES020522, ES015991, ES007148, and ES005022], and the National Institute of Neurological Disorders and Stroke [Grant NS072097], components of the National Institutes of Health.

Reprint Requests

Lauren Aleksunes, Pharm.D., Ph.D.

Department of Pharmacology and Toxicology

Rutgers University

170 Frelinghuysen Rd.

Piscataway, NJ, 08854, USA

Phone: (848) 445-5518

Fax: (732) 445-0119

E-mail: aleksunes@eohsi.rutgers.edu

[1] These two authors contributed equally as corresponding authors.

Figure Legends

Figure 1. Functional characterization of efflux transporters in resting microglia. The ability of BV-2 microglia to efflux fluorescent substrates for specific transporters was evaluated using the Nexcelom Cellometer Vision. A) Fluorescent dyes known as specific ABC transporter substrates were used to characterize function. Specific inhibitors (PSC833, MK-571, KO143) were used as positive controls for functional inhibition. B) Representative fluorescent images of resting microglia incubated with ABC efflux transporter substrates or substrate plus inhibitor. Data (bar graphs) are presented as mean relative fluorescence ± SE (n=3) normalized to cell size. Asterisks (*) represent statistically significant differences ($p < 0.05$) compared to control. Line graphs represent the distribution of individual cell fluorescence. Each point represents the mean percent of cells ± SE (n=3) exhibiting a quantity of fluorescence. The number of cells counted for each sample ranged from 200 to 600 cells.

Figure 2. Activation of microglia with LPS. BV-2 cell activation was examined using A) the xCELLigence RTCA DP analyzer before and after LPS activation. Real time impedance measurements demonstrate the attachment (T=-21 to -20) and growth (T=-16 to T=0) of BV-2 microglia as gradual increases in cell impedance. Addition of LPS to microglia occurred at T=0. LPS-treated microglia are in blue and vehicle-treated control cells are in red. Data are presented as mean ± SE (n=4). B) Microglial activation after 12 hour incubation with LPS was confirmed by quantifying pro-inflammatory cytokine mRNA expression. Data were normalized to Rpl13a mRNA and presented as mean relative mRNA expression ± SE (n=4) compared to 0 ng/ml LPS.

JPET Fast Forward. Published on August 31, 2012 as DOI: 10.1124/jpet.112.196543
This article has not been copyedited and formatted. The final version may differ from this version.

Dotted line at Y=1 represents control expression. Asterisks (*) represent statistically significant differences ($p < 0.05$) compared to 0 ng/ml LPS.

Figure 3. Functional characterization of efflux transporters in activated microglia. The ability of specific transporters to efflux substrates from activated BV-2 microglia (100 ng/ml LPS for 24 hours) was characterized using fluorescent substrates and the Nexcelom Cellometer Vision. A) Fluorescent dyes known as specific ABC transporter substrates were used to characterize function. Specific inhibitors (PSC833, MK-571, KO143) were used as positive controls for functional inhibition. B) Exogenous and endogenous substrates were also examined for confirmation of transporter function. Data (bar graphs) are presented as mean relative fluorescence ± SE (n=3) normalized to cell size. Asterisks (*) represent statistically significant differences ($p < 0.05$) compared to control. Line graphs represent the distribution of individual cell fluorescence. Each point represents the mean percent of cells ± SE (n=3) exhibiting a quantity of fluorescence. The number of cells counted for each sample ranged from 500 to 2000 cells.

Figure 4. mRNA expression of efflux transporters in activated microglia. Relative efflux transporter mRNA was determined after 12 hour incubation of BV-2 microglia with LPS. Data were normalized to Rpl13a and presented as mean relative mRNA expression ± SE (n=4). Asterisks (*) represent statistically significant differences ($p < 0.05$) compared to control. Dotted line at Y=1 represents control expression.

Figure 5. Protein expression of efflux transporters in activated microglia. Relative expression of efflux transporter protein was determined after 24 hours of BV-2 microglial activation with LPS. Semi-quantitative expression of protein was determined by densitometry from western blots. Representative western blots exhibit changes in protein expression. Gapdh was used as loading control. Data are presented as mean relative protein expression ± SE (n=3). Asterisks (*) represent statistically significant differences ($p < 0.05$) compared to control. Dotted line at Y=1 represents control expression.

Figure 6. Indirect immunofluorescence of efflux transporters in activated microglia. BV-2 microglia were grown on chamber slides and incubated with vehicle or 100ng/ml LPS for 24 hours. Slides were fixed in 4% paraformaldehyde and incubated with primary antibodies specific for each efflux transporter and appropriate fluorescent AlexaFluor488-labeled secondary antibodies (*green*). Nuclei (*blue*) were stained with DAPI. Bar = 10μm.

Figure 7. Expression of inflammatory cytokines in activated microglia following NF-κB inhibition. BV-2 microglia were incubated with vehicle or 5μM BAY 11-7082 30 minutes prior to the addition of vehicle or 100ng/ml LPS. Cells were collected after 12 hours and cell lysates were analyzed for mRNA expression of A) IL-1β, B) IL-6, and C) TNFα. D) Cell culture medium was analyzed for TNFα protein by ELISA. mRNA data were normalized to Rpl13a mRNA and presented as mean relative mRNA expression ± SE (n=3). Protein data are presented as mean protein levels ± SE (n=3). Single dagger (†) indicates that protein concentration was below the detection level of 3 pg/mL (ND). Asterisks (*) represent statistically significant differences ($p < 0.05$) compared to control cells (no LPS, no BAY 11-7082). Double dagger (‡)

represents statistically significant differences ($p < 0.05$) compared to LPS-treated cells (no BAY 11-7082).

Figure 8. Expression of Mdr1a/1b and Bcrp mRNA in activated microglia following NF-κB inhibition. BV-2 microglia were incubated with 5μM BAY 11-7082 or DMSO 30 minutes prior to the addition of vehicle or 100ng/ml LPS. Cells were collected after 12 hours and cell lysates were analyzed for mRNA expression of Mdr1a, Mdr1b, and Bcrp. mRNA data were normalized to Rpl13a mRNA and presented as mean relative mRNA expression ± SE (n=3). Dotted line at Y=1 represents control expression. Asterisks (*) represent statistically significant differences ($p < 0.05$) compared to control cells (no LPS, no BAY 11-7082). Double dagger (‡) represents statistically significant differences ($p < 0.05$) compared to LPS-treated cells (no BAY 11-7082).

Figure 9. Expression of Mrp and Nrf2 mRNA in activated microglia following NF-κB inhibition. BV-2 microglia were incubated with 5μM BAY 11-7082 or DMSO 30 minutes prior to the addition of vehicle or 100ng/ml LPS. Cells were collected after 12 hours and cell lysates were analyzed for mRNA expression of Nrf2, the Nrf2 responsive gene, Nqo1, and the efflux transporters Mrp1 and Mrp5. mRNA data were normalized to Rpl13a mRNA and presented as mean relative mRNA expression ± SE (n=3). Dotted line at Y=1 represents control expression. Asterisks (*) represent statistically significant differences ($p < 0.05$) compared to control cells (no LPS, no BAY 11-7082). Double dagger (‡) represents statistically significant differences ($p < 0.05$) compared to LPS-treated cells (no BAY 11-7082).

JPET Fast Forward. Published on August 31, 2012 as DOI: 10.1124/jpet.112.196543
This article has not been copyedited and formatted. The final version may differ from this version.

Table 1. Fluorescent substrates and inhibitors

Substrate	Concentration	Source
Rhodamine 123	5 μM	Sigma-Aldrich (St. Louis, MO)
Calcein AM	2 μM	Sigma-Aldrich (St. Louis, MO)
Hoechst 33342	10 μM	Sigma-Aldrich (St. Louis, MO)
BODIPY Prazosin	2 μM	Invitrogen/Molecular Probes (Eugene, OR)
NBD-Ceramide	5 μM	Avanti Polar Lipids (Alabaster, AL)

Inhibitor	Concentration	Source
PSC833	1 μM	XenoTech LLC (Lenexa, KS)
MK-571	10 μM	Sigma-Aldrich (St. Louis, MO)
KO143	5 μM	Sigma-Aldrich (St. Louis, MO)

JPET Fast Forward. Published on August 31, 2012 as DOI: 10.1124/jpet.112.196543
This article has not been copyedited and formatted. The final version may differ from this version.

Table 2. Normalized mRNA expression of efflux transporters in resting BV-2 microglia

Gene	Ct Value Microglia	Percent Difference from Liver[1]
Mrp1	21.8	8029.2%
Mrp2	26.4	0.4%
Mrp3	23.7	6.3%
Mrp4	24.5	5509.9%
Mrp5	22.8	304.6%
Mdr1a	22.6	776.5%
Mdr1b	22.6	1279.0%
Bcrp	24.1	9.6%

[1]Basal expression of BV-2 microglial mRNA was compared to C57BL/6 mouse liver and normalized to the reference gene, Rpl13a.

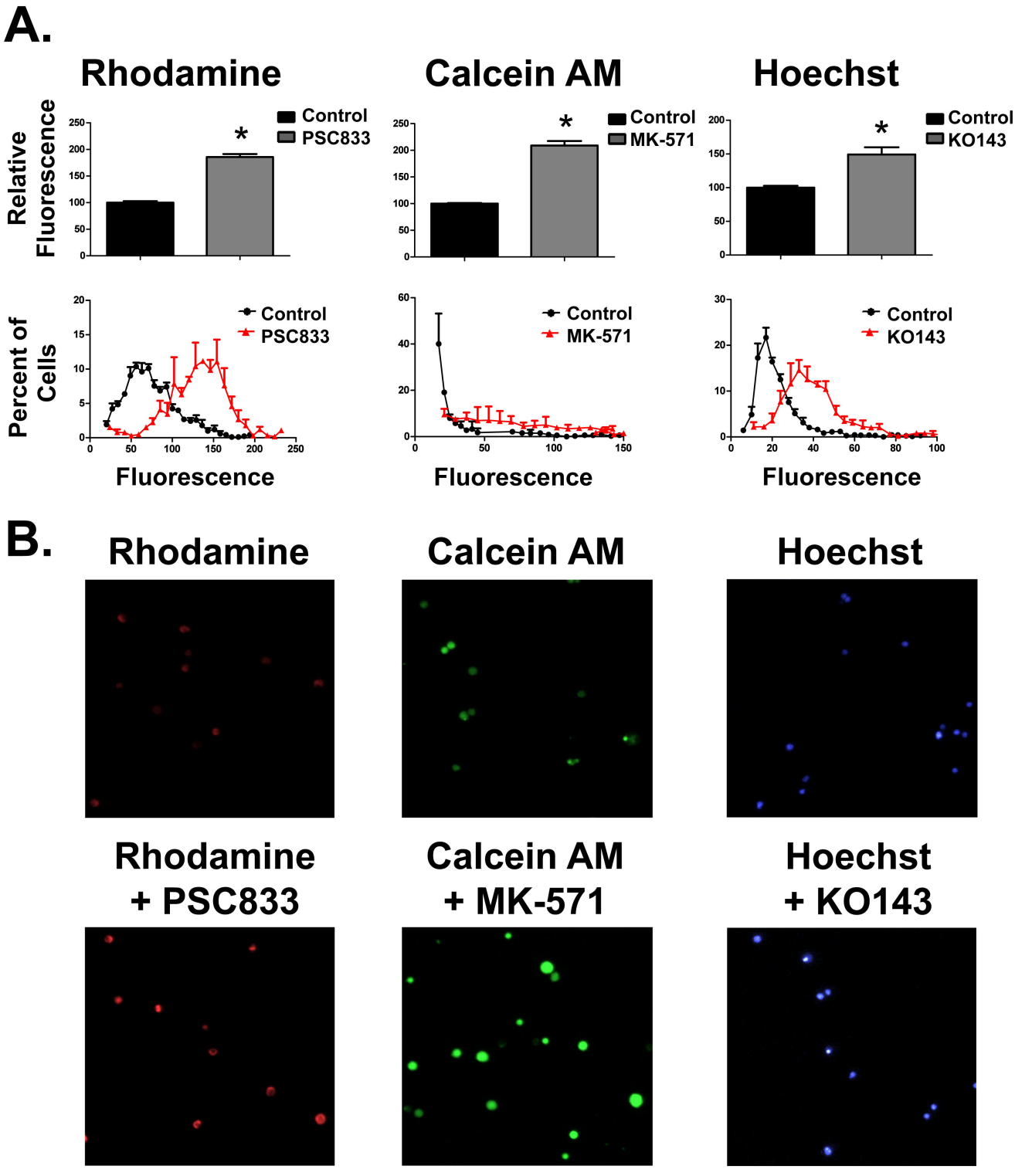
A.
Rhodamine
Calcein AM
Hoechst
Relative Fluorescence
Control
PSC833
MK-571
KO143
*
Percent of Cells
Fluorescence
B.
Rhodamine
Calcein AM
Hoechst
Rhodamine + PSC833
Calcein AM + MK-571
Hoechst + KO143

Fig. 1.

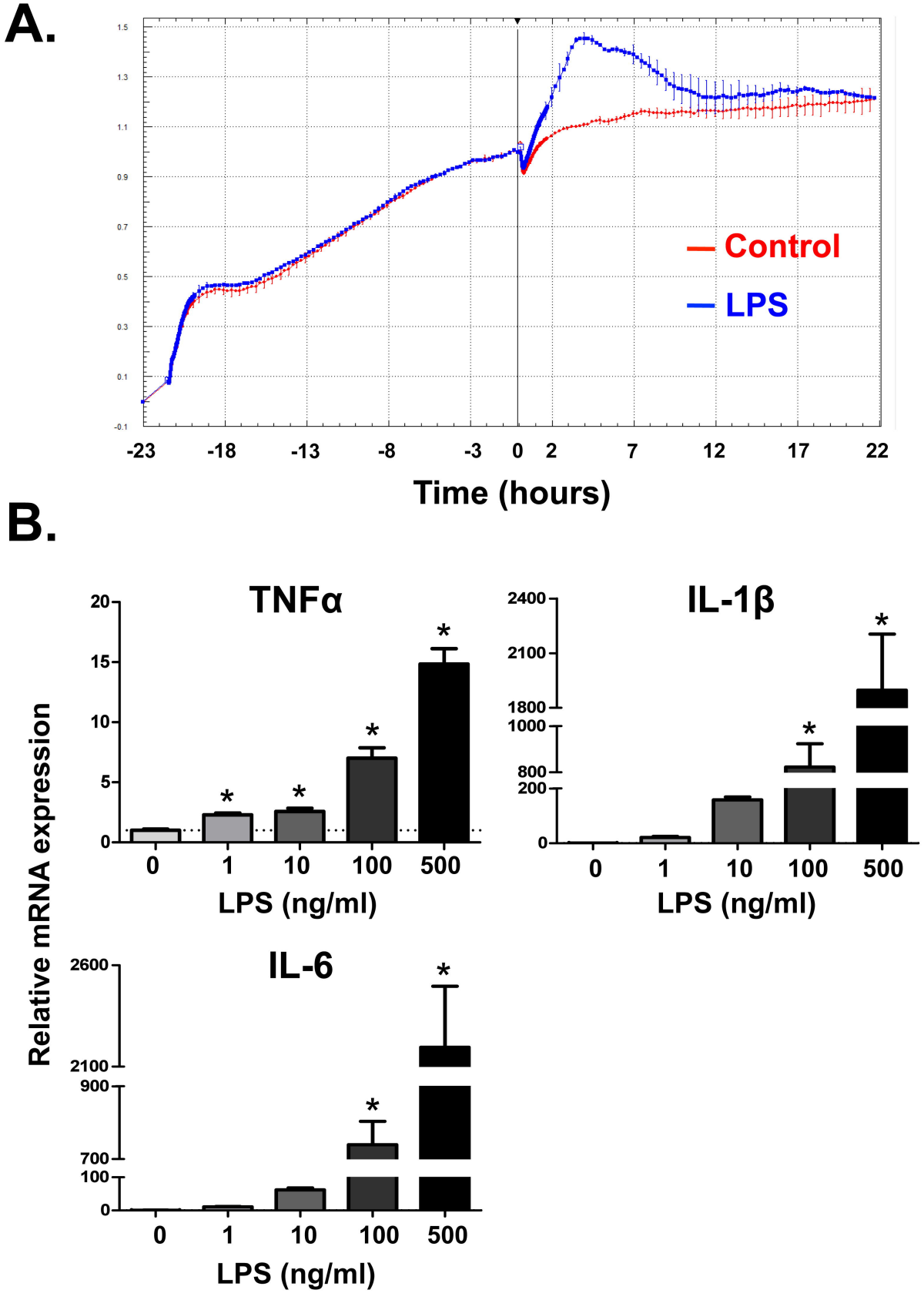
A.
Control
LPS
Time (hours)
B.
TNFα
IL-1β
IL-6
Relative mRNA expression
LPS (ng/ml)

Fig. 2.

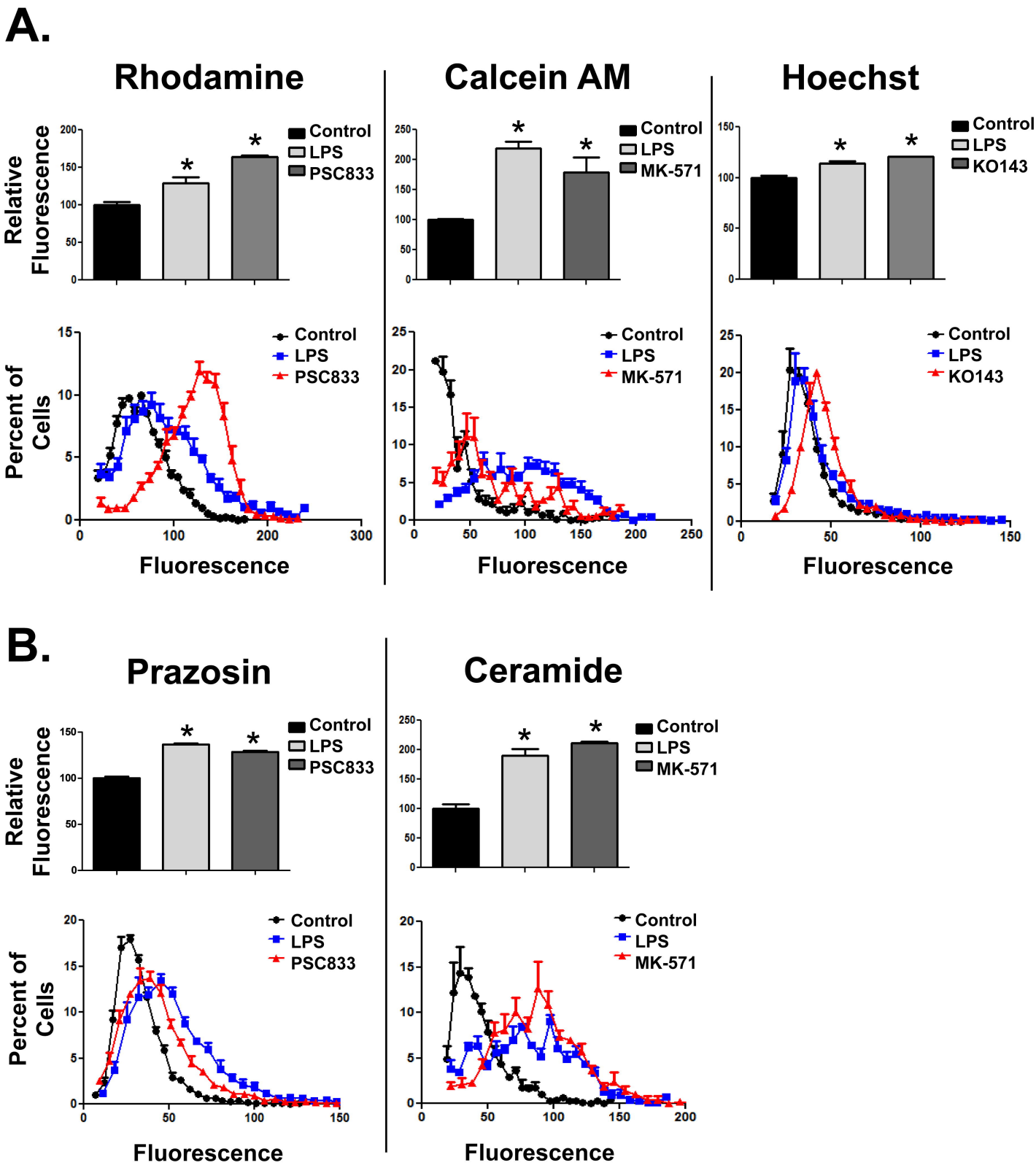
A.
Rhodamine
Calcein AM
Hoechst
Relative Fluorescence
Control
LPS
PSC833
MK-571
KO143
Percent of Cells
Fluorescence
B.
Prazosin
Ceramide

Fig. 3.

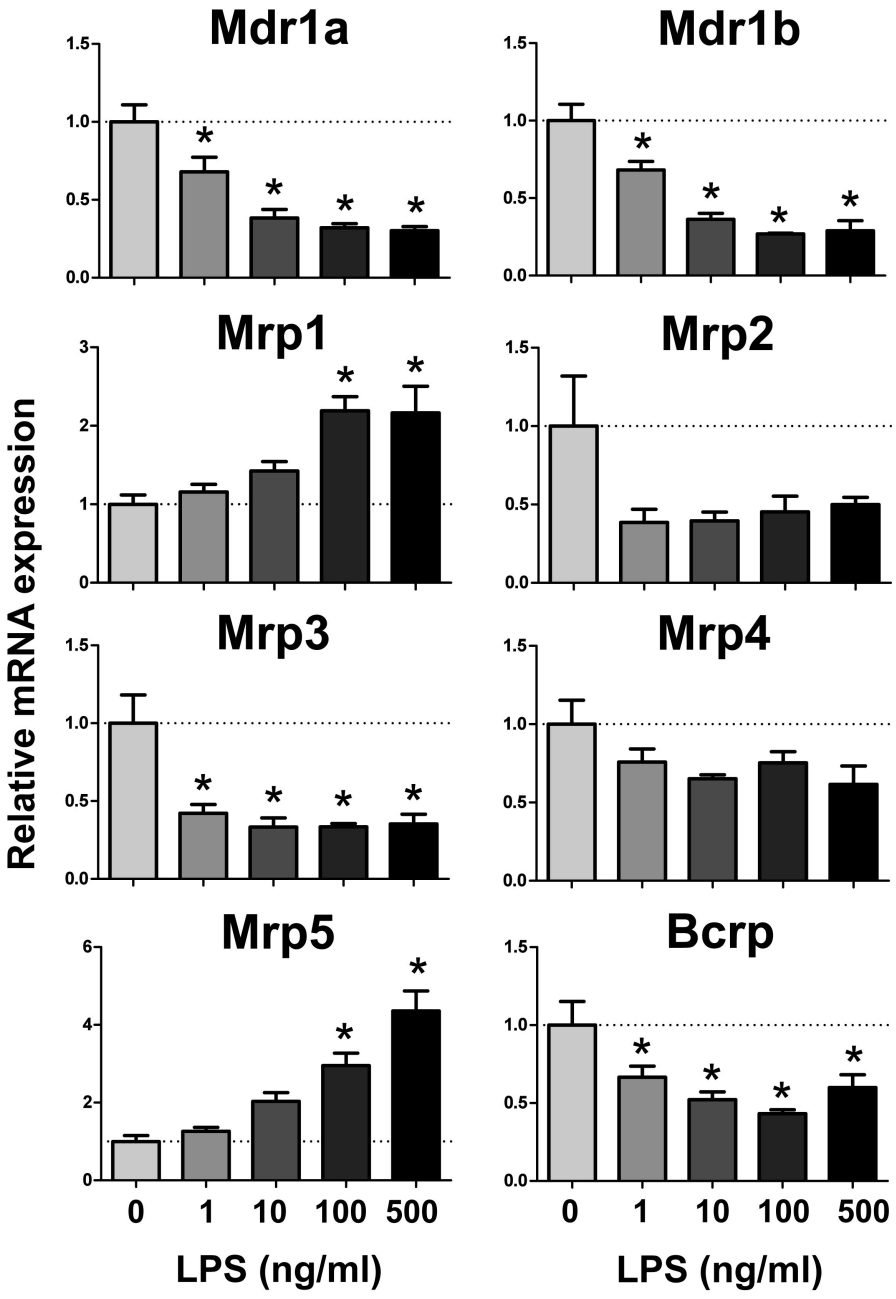
Mdr1a
Mdr1b
Mrp1
Mrp2
Mrp3
Mrp4
Mrp5
Bcrp
Relative mRNA expression
0
1
10
100
500
LPS (ng/ml)
LPS (ng/ml)

Fig. 4.

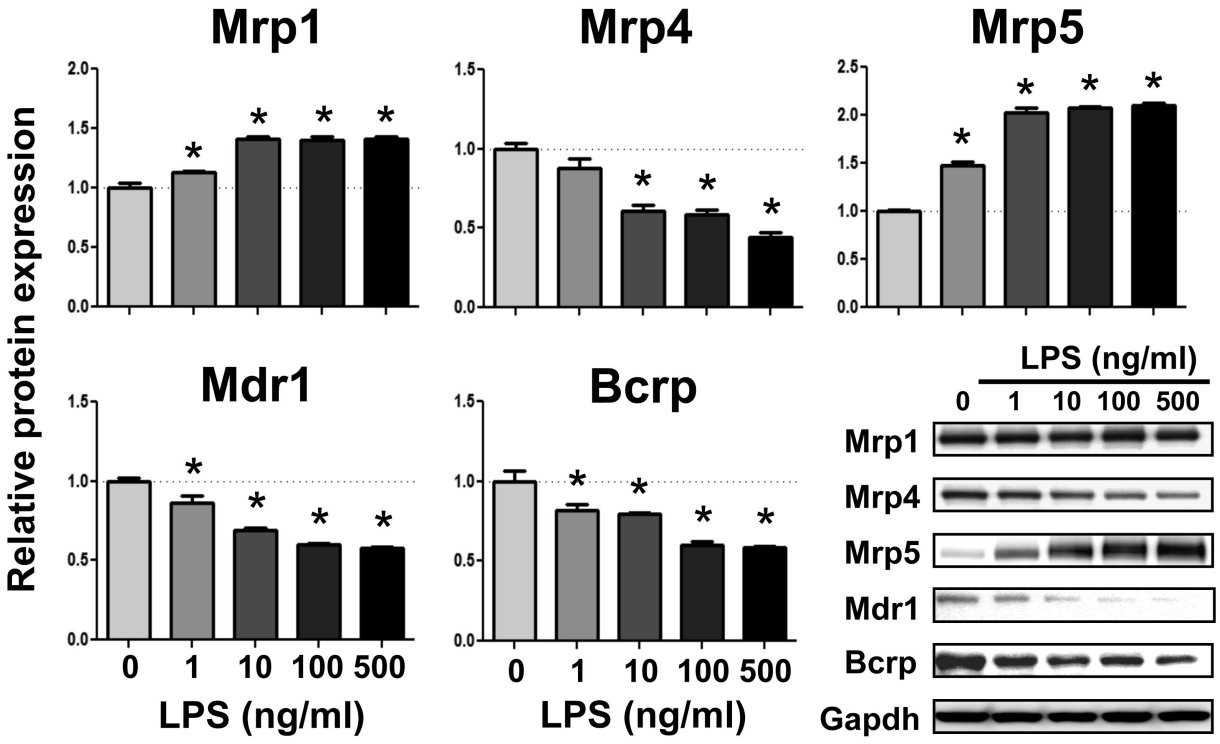
Mrp1
Mrp4
Mrp5
Mdr1
Bcrp
Relative protein expression
LPS (ng/ml)
0 1 10 100 500
Mrp1
Mrp4
Mrp5
Mdr1
Bcrp
Gapdh

Fig. 5

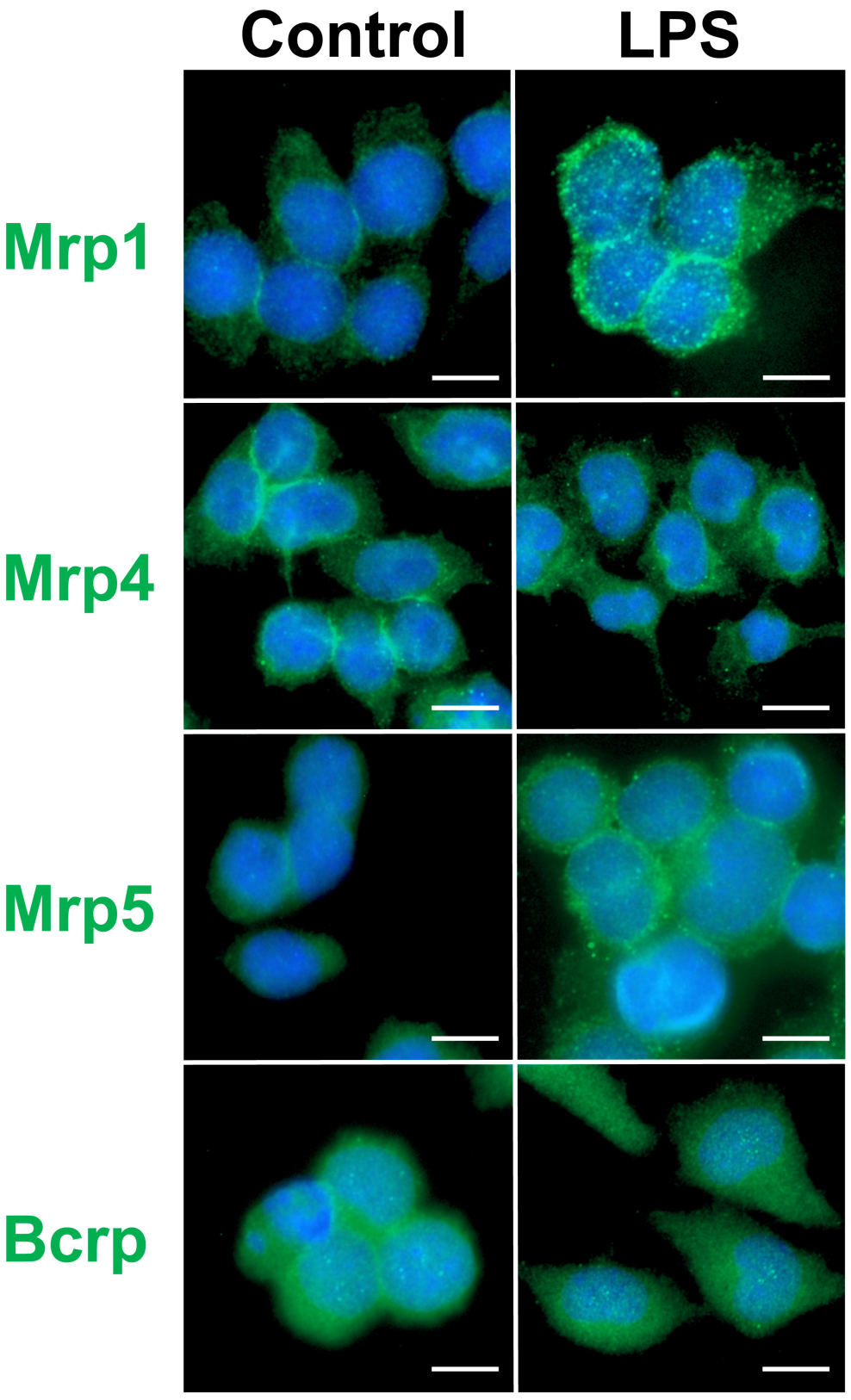

Fig. 6.

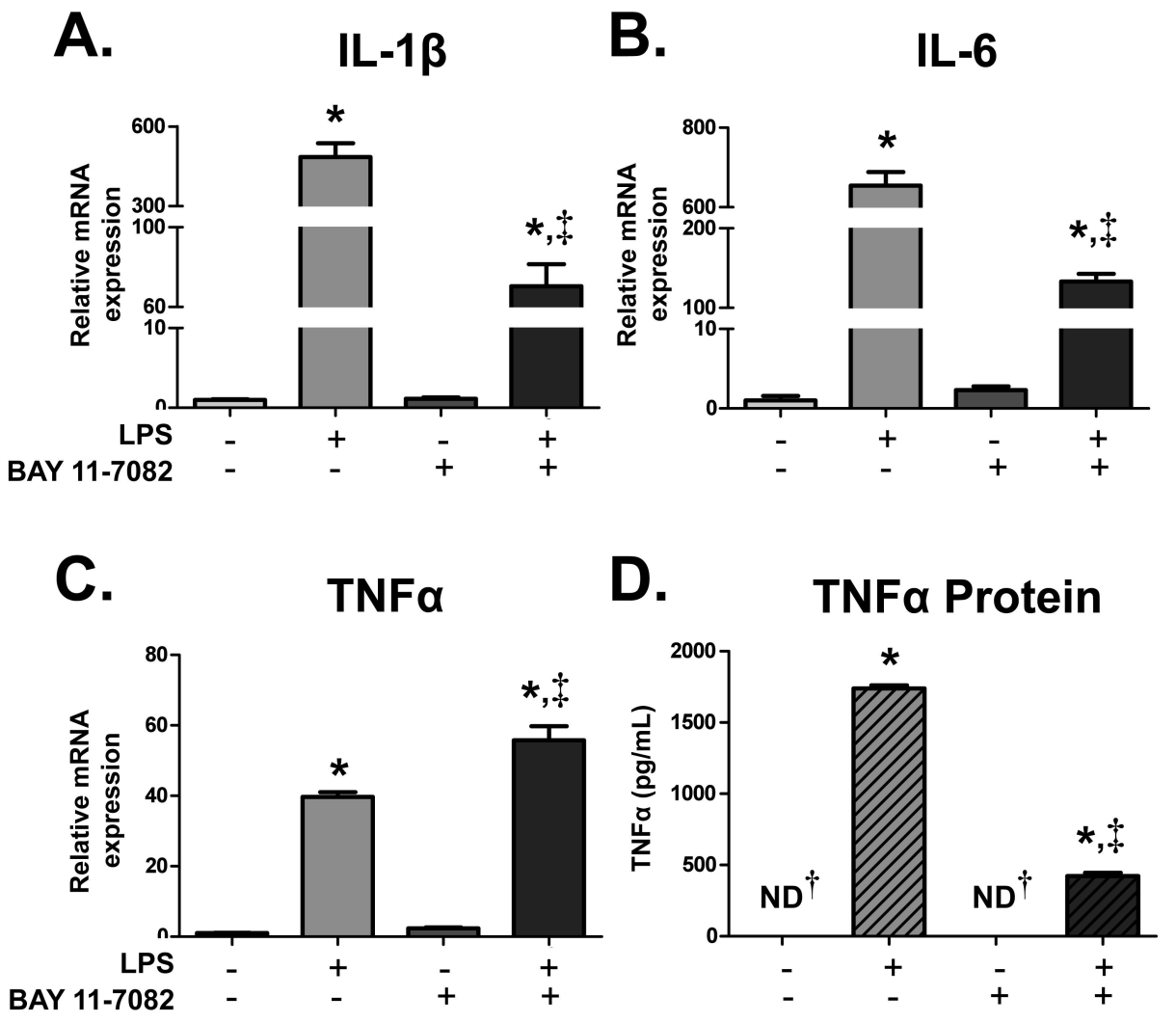
A.
IL-1β
Relative mRNA expression
600
300
100
60
10
0
*
*,‡
LPS - + - +
BAY 11-7082 - - + +
B.
IL-6
Relative mRNA expression
800
600
200
100
10
0
*
*,‡
- + - +
- - + +
C.
TNFα
Relative mRNA expression
80
60
40
20
0
*
*,‡
LPS - + - +
BAY 11-7082 - - + +
D.
TNFα Protein
TNFα (pg/mL)
2000
1500
1000
500
0
*
*,‡
ND†
ND†
- + - +
- - + +

Fig. 7.

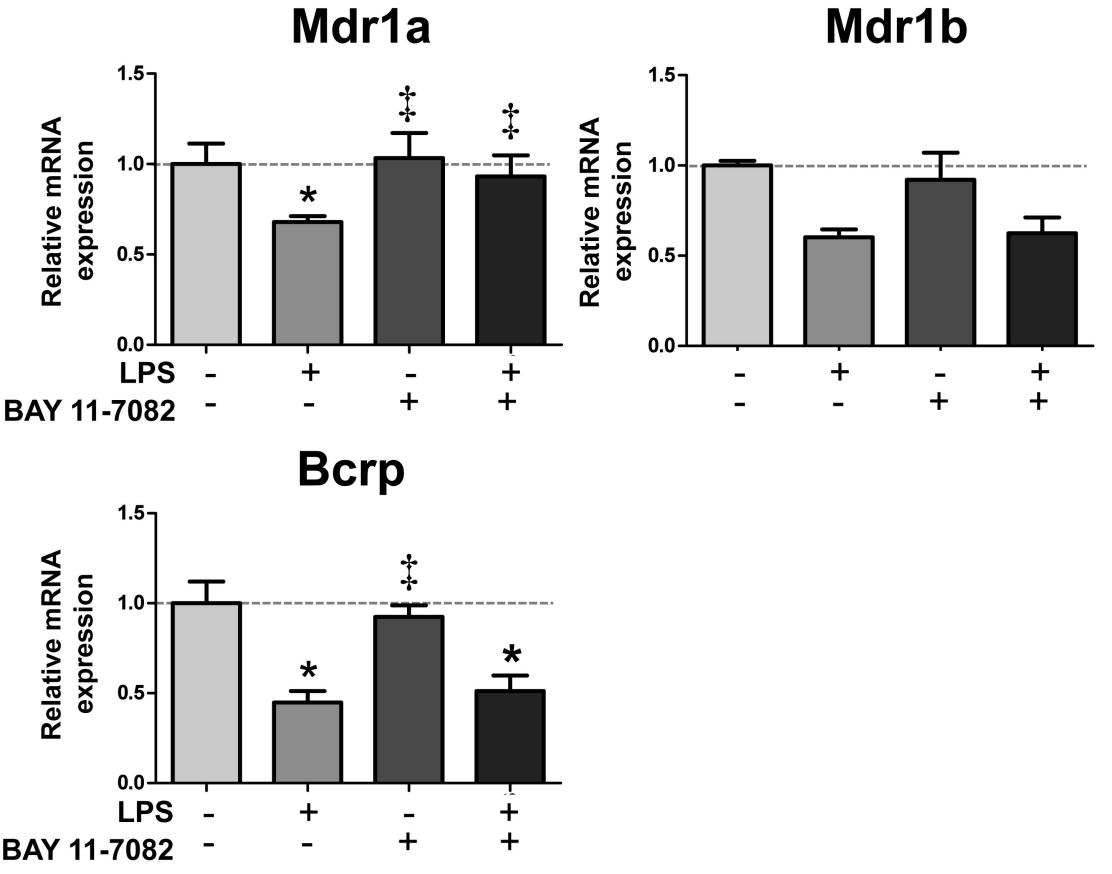
Mdr1a
Relative mRNA expression
1.5
1.0
0.5
0.0
*
‡
‡
LPS - + - +
BAY 11-7082 - - + +
Mdr1b
Relative mRNA expression
1.5
1.0
0.5
0.0
- + - +
- - + +
Bcrp
Relative mRNA expression
1.5
1.0
0.5
0.0
*
‡
*
LPS - + - +
BAY 11-7082 - - + +

Fig. 8.

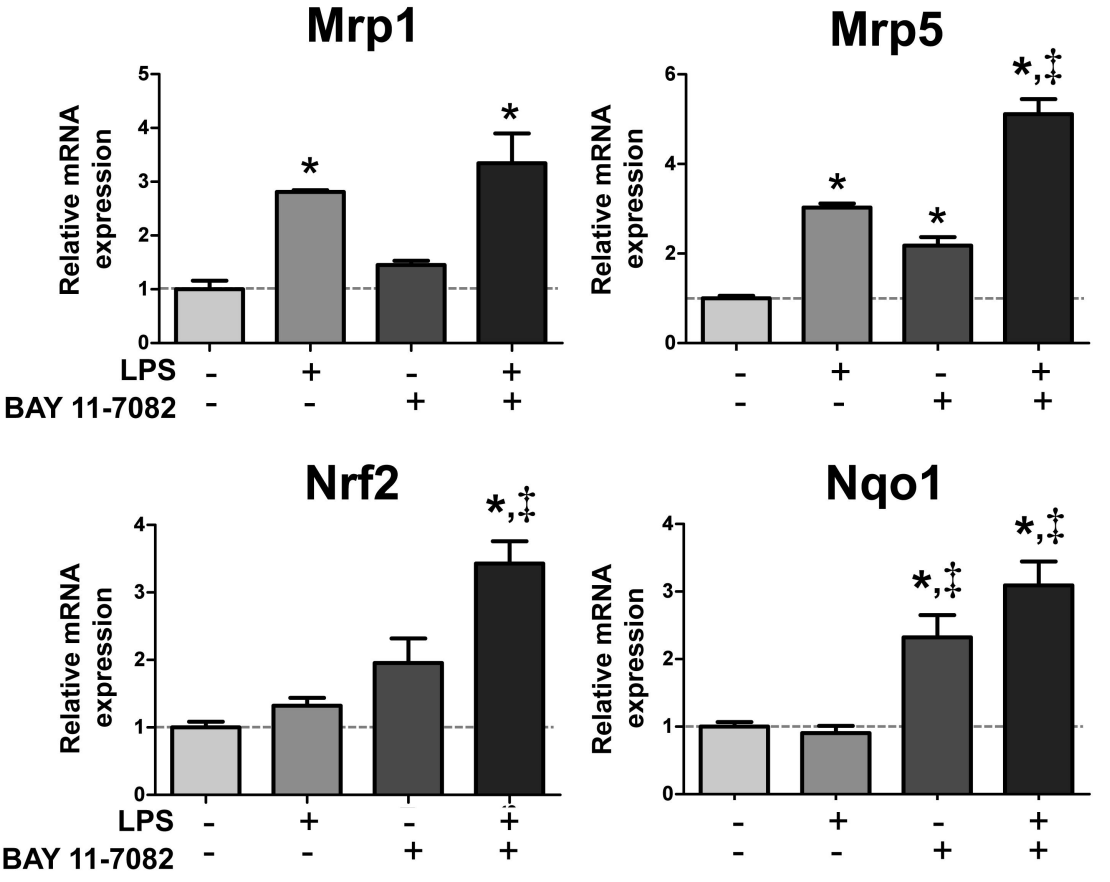
Mrp1
Mrp5
Nrf2
Nqo1
Relative mRNA expression
LPS
BAY 11-7082
*
*,‡

Fig. 9.

Inflammatory Regulation of ABC Efflux Transporter Expression and Function in Microglia

Christopher J. Gibson, Muhammad M. Hossain,
Jason R. Richardson, Lauren M. Aleksunes

Journal of Pharmacology & Experimental Therapeutics

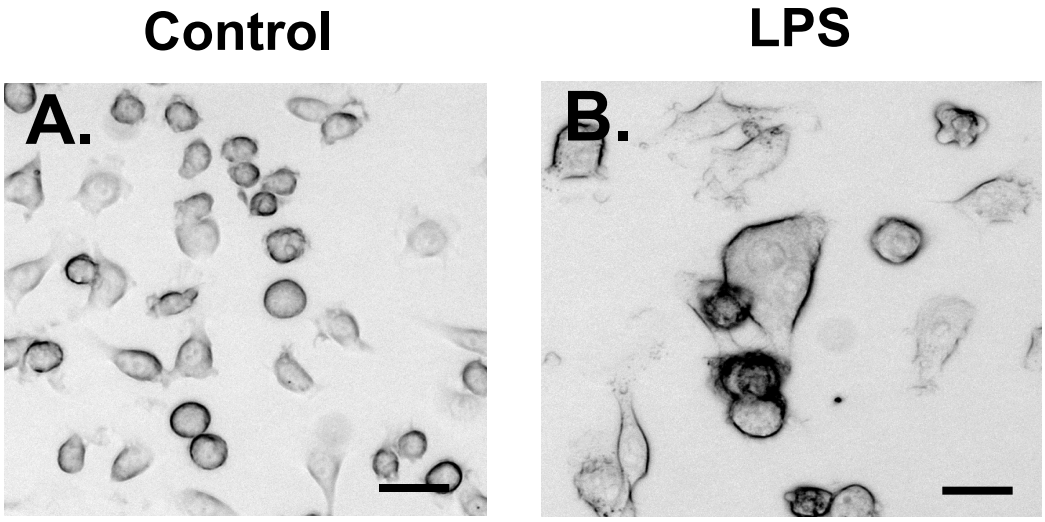

Supplemental Figure 1. BV-2 microglia morphology. Confirmation of altered morphology was determined visually (T = 6 hours) by examining live cell cultures grown in A) fresh medium or B) 100 ng/ml LPS. Bar = 20μm.

Inflammatory Regulation of ABC Efflux Transporter Expression and Function in Microglia

Christopher J. Gibson, Muhammad M. Hossain,
Jason R. Richardson, Lauren M. Aleksunes

Journal of Pharmacology & Experimental Therapeutics

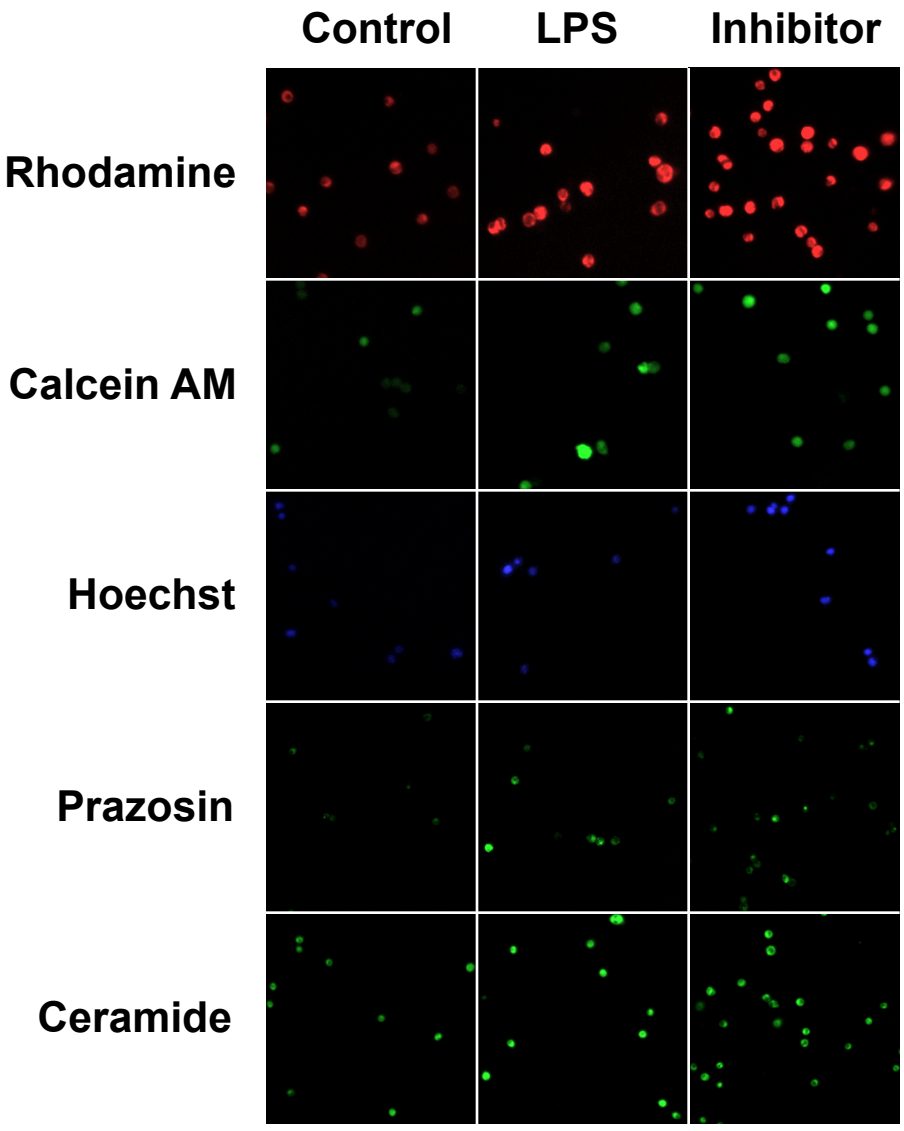

Supplemental Figure 2. Intracellular retention of fluorescent substrates in activated microglia. Representative fluorescent images of activated BV-2 microglia incubated with ABC efflux transporter substrates (*LPS*) or control BV-2 microglia incubated with substrate (*Control*) or substrate plus inhibitor (*Inhibitor*).

Inflammatory Regulation of ABC Efflux Transporter Expression and Function in Microglia

Christopher J. Gibson, Muhammad M. Hossain,
Jason R. Richardson, Lauren M. Aleksunes

Journal of Pharmacology & Experimental Therapeutics

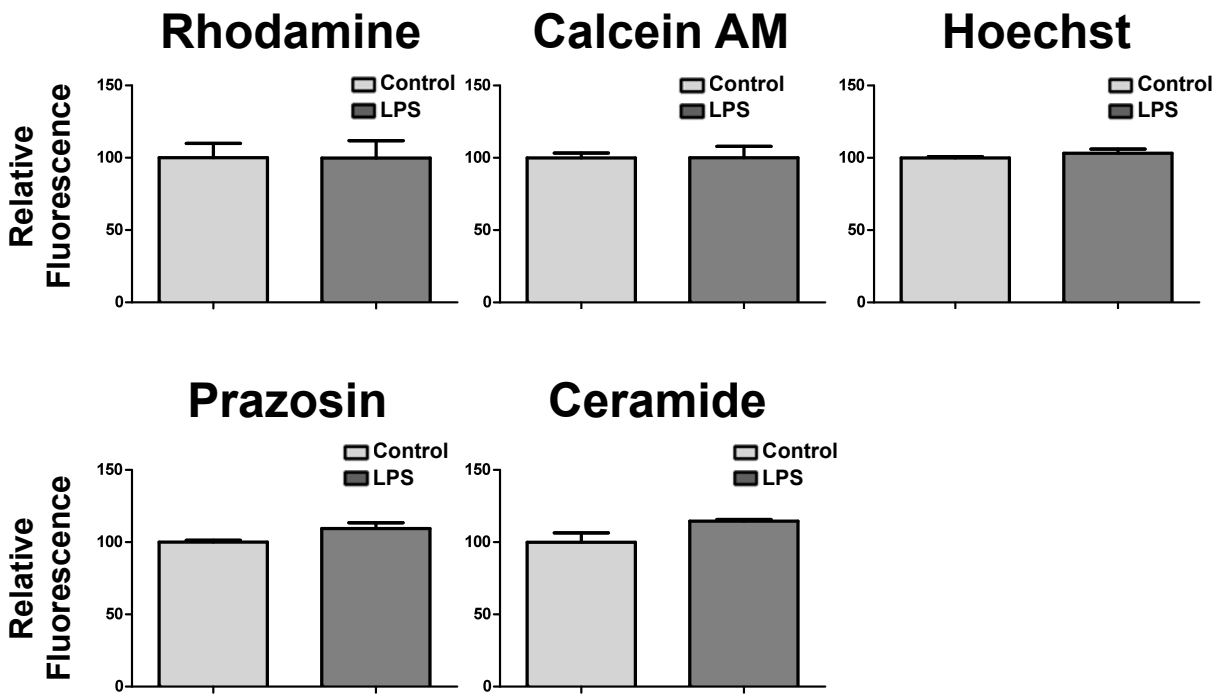

Supplemental Figure 3. Cellular uptake of fluorescent substrates. *The relative amount of fluorescent substrate uptake in control and activated BV-2 microglia (100 ng/ml LPS for 24 hours) was quantified using the Nexcelom Cellometer Vision. Cellular fluorescence was measured immediately following a 30 minute incubation with each substrate. Data are presented as mean relative fluorescence ± SE (n=3) normalized to cell size. There was no statistical difference ($p < 0.05$) in the amount of fluorescent substrate uptake between control and LPS -activated microglia.*

Inflammatory Regulation of ABC Efflux Transporter Expression and Function in Microglia

Christopher J. Gibson, Muhammad M. Hossain,
Jason R. Richardson, Lauren M. Aleksunes

Journal of Pharmacology & Experimental Therapeutics

Supplemental Table 1. qPCR primer sequences

Target	Forward Primer (5' → 3')	Reverse Primer (5' → 3')
TNFα[a]	*AGCCCACGTCGTAGCAAACCAC*	*AGGAGCACGTAGTCGGGGCA*
IL-1β[b]	*GACCTTCCAGGATGAGGACA*	*AGCTCATATGGGTCCGACAG*
IL-6[b]	*AGTTGCCTTCTTGGGACTGA*	*CAGAATTGCCATTGCACAAC*
Rpl13a[a]	*CTGTGAAGGCATCAACATTTCTG*	*GACCACCATCCGCTTTTTCTT*
Mdr1a/Abcb1a[a]	*TGCCCCACCAATTTGACACCCT*	*ATCCAGTGCGGCCTGAACCA*
Mdr1b/Abcb1b[a]	*GTGTTAAAGGGGCGATGGGCG*	*AGGCTTGGCCAGACAACAGCTT*
Mrp1/Abcc1[a]	*GCTGTGGTGGGCGCTGTCTA*	*CCCAGGCTCAGCCACAGGAA*
Mrp2/Abcc2[b]	*AGCAGGTGTTCGTTGTGTGT*	*AGCCAAGTGCATAGGTAGAGAAT*
Mrp3/Abcc3[b]	*CTGGGTCCCCTGCATCTAC*	*GCCGTCTTGAGCCTGGATAAC*
Mrp4/Abcc4[b]	*CCAGACCCTCGTTGAAAGAC*	*TGAAGCCGATTCTCCCTTC*
Mrp5/Abcc5[a]	*AGGGCAGCTTGTGCAGGTGG*	*TGCTGTTCCCGCTTCCTTGCT*
Bcrp/Abcg2[a]	*GCGGAGGCAAGTCTTCGTTGC*	*TCTCTCACTGTCAGGGTGCCCA*
Nrf2	*TCTTGGAGTAAGTCGAGAAGTGT*	*GTTGAAACTGAGCGAAAAAGGC*
Nqo1	*AGGATGGGAGGTACTCGAATC*	*AGGCGTCCTTCCTTATATGCTA*

[a] Integrated DNA Technologies, Coralville, IA
[b] University of Rhode Island, Kingston, RI, Dr. Angela Slitt